Electronic Supplementary Information

Towards highly integrated CO_2 capture and conversion: Direct synthesis of cyclic carbonates from industrial flue gas.

Alexander Barthel,[a,b] Youssef Saih,[a] Michel Gimenez,[c] Jérémie Pelletier,[a] F. E. Kühn,[b] Valerio D´Elia*[a,d] and Jean-Marie Basset*[a]

[a]*King Abdullah University of Science & Technology, KAUST Catalysis Center (KCC), 23955-6900 Thuwal, Saudi Arabia.*

[b]*Molecular Catalysis, Catalysis Research Center, Ernst-Otto-Fischer-Strasse 1 and Faculty of Chemistry, Lichtenbergstrasse 4, Technische Universität München, D-85747 Garching bei München (Germany)*

[c]*LafargeHolcim - CIP/IPS - 95, rue du Montmurier, 38291 Saint-Quentin-Fallavier, France*

[d]*Department of Materials Science and Engineering, Vidyasirimedhi Institute of Science and Technology, 21210, Wang Chan, Rayong, Thailand.*

Table of contents

1. General information and materials

All manipulations of air-sensitive materials were carried out in a glovebox or under a protective argon atmosphere using Schlenk techniques. The epoxides were purchased from Sigma Aldrich (propylene oxide, 1,2-epoxybutane, epichlorohydrin purity: ≥ 99.0 %; cyclohexene oxide purity: 98 %; styrene oxide purity: 97 %) and generally used as received. For those experiments where distilled epoxides were used, propylene oxide and epichlorohydrin were stirred overnight over CaH_2 and distilled. Tetrabutylammonium bromide (TBAB, Sigma Aldrich, ≥ 99.0 %) was molten at 100 – 150°C in a Schlenk tube, stirred under vacuum for at least 4 hours and stored under protective atmosphere. Metal halides were purchased from Strem Chemicals (YCl_3 99.9 %; $ScCl_3$ 99.99 %) or Sigma Aldrich ($NbCl_5$; 99.995; $ZrCl_4$; ≥ 99.5 %) with a purity of 99.5% or higher and used without further purification. Carrier gases (Ar, grade 5.0, ≥ 99.999 %; O_2, grade 4.5, ≥ 99.995 %) and pure CO_2 (grade 2.5, ≥ 99.5 %; H_2O ≤ 32 ppm) were purchased from Abdullah Hashim Industrial gases & Equipment (AHG) and used as received.

^1H NMR Spectra were recorded in $CDCl_3$ on an automated 400 MHz Bruker Biospin instrument, chemical shifts are reported in ppm (δ, relative to TMS) using $CHCl_3$ residual peak (δ = 7.26 ppm) in $CDCl_3$ as an internal standard. In-situ IR spectroscopy was performed with a Mettler Toledo ReactIR 45 equipped with a DiComp diamond probe in a regular 2 neck-flask with valve. The gas flow was regulated by means of Bronkhorst EL-Flow Select Mass flow controllers, operated via PC using Bronkhorst FlowView software or, alternatively, by Aalborg GFC mass flow controllers operated through a 4-channels Aalborg Command DPROC Module.

2. Experimental procedure setup for the synthesis of cyclic carbonates

In a typical experiment, an oven-dried two-necked round bottom flask equipped with a Schlenk valve and a Teflon stirrer was placed inside a glovebox. YCl_3 (249 mg, 1.275 mmol, 1 mol %), TBAB (822 mg, 2.55 mmol, 2 mol %) were added to the flask. The flask necks were sealed with a glass stopper and a rubber septum and the flask was removed from the glove box. The reaction flask was placed in an ice bath and epichlorohydrin (10 mL, 11.8 g, 127.5 mmol) was added via syringe. The mixture was stirred for 10 - 15 min at room temperature till complete dissolution of the solid material. The clear reddish solution was connected to the set up in figure S1: the *in situ* IR probe was inserted in the flask under a flow of pure Ar or O_2 (from the Schlenck valve) and contacted with the reaction mixture. A needle, connected to the CO_2 source (still not active), was dipped into the solution, whereas the Schlenck valve was

connected to a bubble-counter to serve as a monitor for the gas flow. A total gas flow of 8 sccm (1 sccm: $7.43 \cdot 10^{-7}$ mol/s) was bubbled through the solution for 5 h. The flow volume was obtained by mixing the individual flows from a CO_2 and an Ar (or O_2) cylinder. The individual flow of each gas was regulated via periodically calibrated mass-flow controllers. In the case of the catalytic runs employing industrial flue gas, the gas source was represented by the lecture bottle containing flue gas. This was connected to the reaction flask in the same way as the pure gases. In this case, a single mass flow controller was used, regulating a flow of 8 sccm flue gas from the lecture bottle. Following reaction, a sample of the reaction mixture was withdrawn to determine conversion.

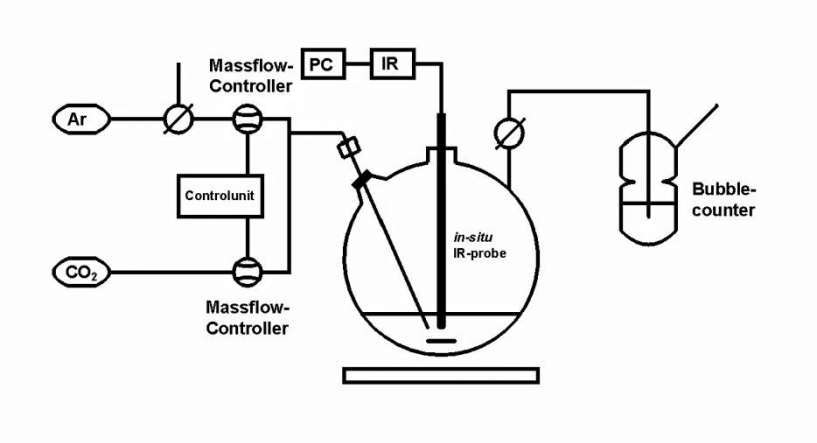

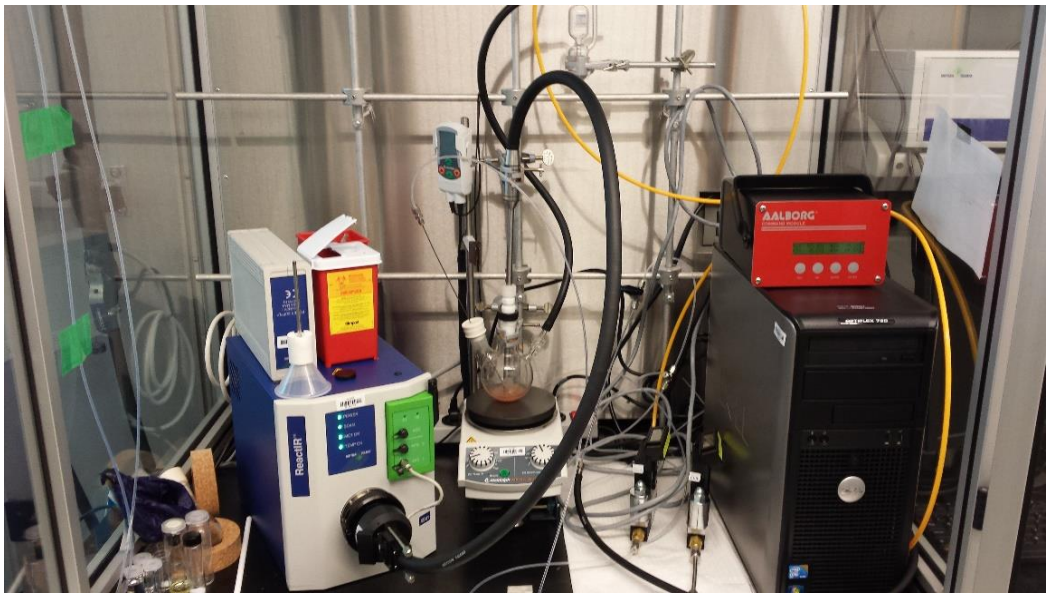

Figure S1. (Top) Schematic experimental setup for the synthesis of cyclic carbonates from CO_2 and epoxides under flow conditions. (Middle) Photography of the experimental set up during reaction. (Bottom) Photography of the experimental set-up when using flue gas (in the lecture bottle) as a CO_2 source.

3. Sampling of flue gas

The flue gas samples were collected at a height of approximately 60 m from the fume stack of the Lafarge-Al Safwa cement factory, located at the Farasan Mountains of the Kingdom of Saudi Arabia (22.553972° N, 39.435464° E, See Figure S2) and were stored at 23 °C into 450 mL carbon-steel lecture bottles geared with a brass CGA 110/180 valve at a pressure of 5 to 7 bar for not longer than a week. Sampling was carried out from a service hatch using a self-built setup consisting of a rudimental glass wool filter system, Swagelok piping and an "ad-hoc"s modified compressor (operating up to 8 bar) that was used to withdraw, compress and store the flue gas withdrawn from the fume stack prior to transfer to the lecture bottles through a venting valve (See Figure S3, Left). The flue gas composition at the source of sampling was controlled via an industrial gas analyzer (Figure S3, Right) that was used also to control the concentration of the flue gas prior utilization in the laboratory (See Table S1).

Table S1: Composition of the flue gas sampled at Al Safwa using the setup displayed in Fig. S3, Right

Component	Concentration
O_2	7.7 %
CO_2	10.2 % (v/v)
CO	0.1 % (v/v)
NO_x[a]	400 mg/m^3
SO_x	300 mg/m^3
H_2O	2 % (v/v)

[a] NO/NO_2 ratio and SO_2/SO_3 ratio ca. 20:1.

Figure S2. (Left) The fume stack of the Lafarge-Al Safwa cement factory from where the flue gas was sampled at a height of about 60 m (Right) Sampling flue gas from a service hatch of the fume stack *via* a self-made set-up described in Figure S3.

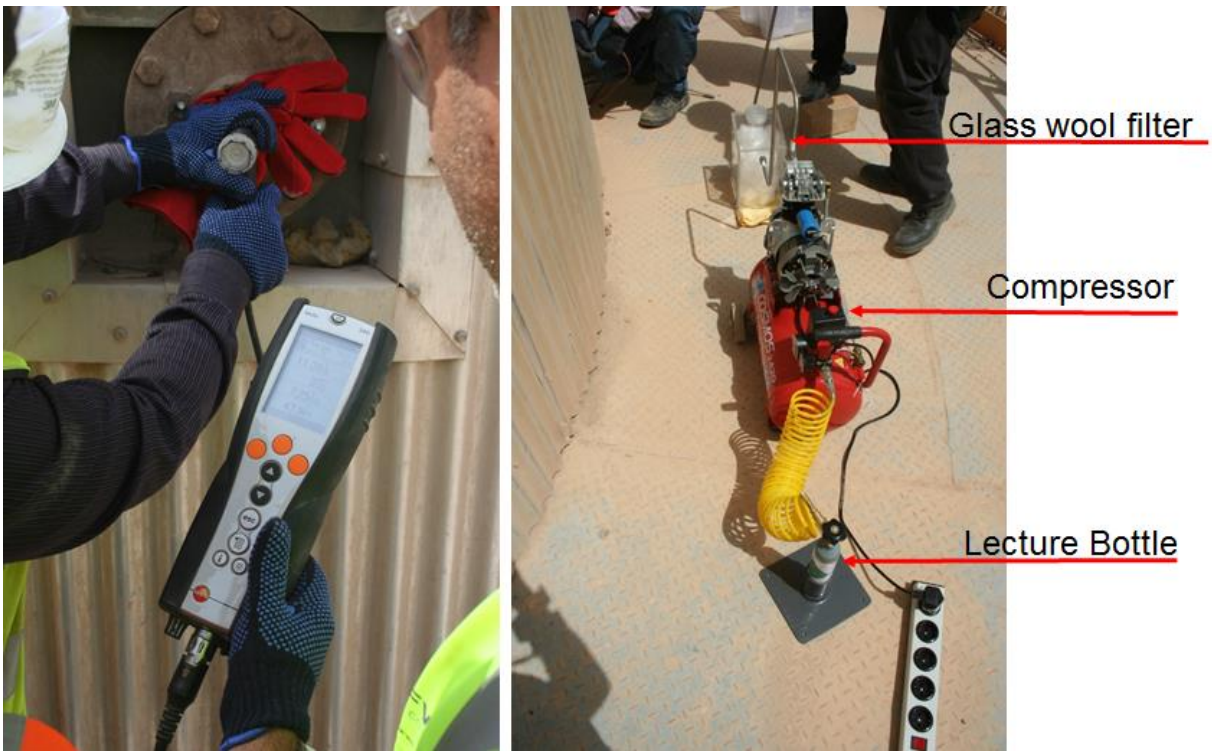

Figure S3. (Left) The composition of the flue gas at the source and after sampling was controlled by means of an industrial gas analyzer. (Right) Detailed view of the sampling setup constituted of 3 parts: an air tight plexiglas box filled with glass wool to prevent fly ashes to reach the compressor; a modified compressor able to withdraw flue gas through the Swagelok pipe installed in its engine and to store it at a pressure of ca. 8 bar; lecture bottles connected to the venting valve of the compressor used to store and transport the flue gas for laboratory use.

The composition of the flue gas samples collected at the point source is the result of a series of processes. The first process leading to an output of CO_2 in the plant is the calcination step that produces the desired CaO from $CaCO_3$ with CO_2 as a side-product. At Al-Safwa $CaCO_3$ is ground through a wind-swept ball mill creating the right particle size for wind-transport and calcination at the kiln. The calcination step would provide a CO_2 content of almost 100% and, therefore, sampling flue gas just after calcination would be an ideal way to obtain highly pure and concentrated CO_2 displaying faster reaction kinetics. Nevertheless, the high temperatures of both the flue gas and of the actual kiln-components (900 °C) make it very challenging under a technical standpoint and would have required more elaborated and expensive sampling devices. Following the calcination, the ensuing flue gases are combined with the flue gases produced from the combustion of heavy fuel oils (HFO; fuel composition: C, 84 %; H, 13 %; S, 3%) necessary for heating and energy production. This lowered the CO_2 content along the stream. The combined flue gas of both processes is led to the chimney, while only a small portion of the flue gas is being recycled as transportation agent of ground particles from the ball mill to the kiln. To decrease the temperature of the flue gas in the chimney, fresh air is introduced in small quantities (10-15 %) at various points, thus finally resulting in a CO_2 concentration between 10 to 12 % in the flue gas at the sampling point, and in an average temperature of 172°C. Although the concentration of CO_2 at the collection point is much lower than that observed at the calcination point, we considered sampling at the fume stack more practical. Moreover, the CO_2 concentration of the collected samples is comparable to that of other major CO_2 emitters such as power stations.

The limitations of the sampling and the synthetic application of industrial flue gas with regards to safety, composition and storage have been discussed by North et al.[27] In our case we noticed that the composition of the flue gas in terms NO_x, SO_x, CO and CO_2 did not vary from the source of sampling to the storage cylinder and it was maintained through time. The composition of the sampled flue gas in terms of moisture (ca. 2 % vol. H_2O) is lower than that measured at the source of sampling (ca. 5 % vol. H_2O) as part of the moisture was unavoidably absorbed/condensed in the glass wool filter used to block the fly ashes particles from reaching the compressor unit (as observed by condensation of water vapor inside the filter case). This is probably due to the cooling of the flue gas below its dew point during the sampling operations. The dependency of the reaction rate on the concentration of water in the epoxide solution is reported in Section 5b of this ESI file.

4. Determination of the conversion

The conversion of epoxides **1a-1e** (epoxide **1f** did not afford the corresponding carbonate product under the reaction conditions) was generally determined via ^{1}H NMR by comparison of the integrals of one of the diastereotopic OC*H*$_2$CHR protons in the starting material (H_a) and in the product (H_b) according to equation (1) and to the chemical shifts in Table S2.

Eq. 1 Conversion calculated from the intensities (I_H) of the corresponding OC*H*$_2$CHR protons in the starting material and in the product.

$$Conversion = \frac{I_{H_b}}{\left(I_{H_a} + I_{H_b}\right)}$$

Table S2 Chemical Shifts (δ, ppm, $CDCl_3$) for the corresponding OC*H*$_2$CHR protons in the epoxides and in the carbonates products (See also the ^{1}H NMR spectra in Section 7).

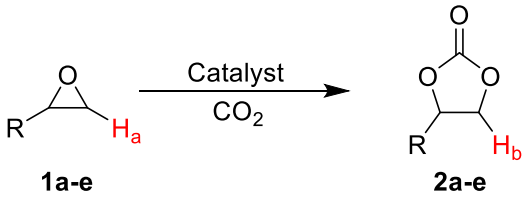

1a-e **2a-e**

R = CH_2Cl (**2a**), R = Me (**2b**), R = Et (**2c**)
R = Bu (**2d**), R = Ph (**2e**)

1/2	H_a (ppm)	H_b (ppm)
1a/2a	2.82	4.56
1b/2b	2.69	4.52
1c/2c	2.72	4.51
1d/2d	2.75	4.55
1e/2e	3.17	4.81

This method could not be applied to the determination of the conversion of epoxide **1b** at room temperature, as partial evaporation of the excess epoxide in the stream of flue gas was observed under these reaction conditions. This led to an overestimation of the epoxide conversion. In this case, the yield of carbonate **2b** was generally determined by isolation of the product: following reaction, slow precipitation of the catalyst was observed upon exposure of the reaction mixture to the environment. After 24 h, the liquid phase was diluted with dichloromethane and the precipitate was removed by filtration. The organic phase was subsequently poured on a plug of silica gel and the fractions containing carbonate **2b** were collected and evaporated under reduced pressure.

In the case of very low **1b** conversion (as in the case of the reactions using diluted CO_2 or flue gas), the residual epoxide was entirely evaporated under reduced pressure. In order to determine the conversion avoiding handling losses a known amount of propylene oxide (3.5 mL, 50 mmol) was added again to the reaction mixture as an internal NMR standard. The molar ratio of propylene carbonate in the mixture (and therefore the amount of propylene carbonate) could be readily determined by the ratio of the integrals of the corresponding protons in the carbonate product and of the known amount of epoxide standard.

5. Additional Catalysis Data

5a. Investigation of the catalytic activity of various metal halides.

The catalysis data presented in Chart 1 of the manuscript (comparison on the catalytic performance of various early transition metal halides) are presented in a table format in Table S3. This includes the data for the apparent initial reaction rates (k_{rel}).

Table S3: Catalytic performance of various metal halides and TBAB in the cycloaddition of CO_2 to epoxide **1a**.[a]

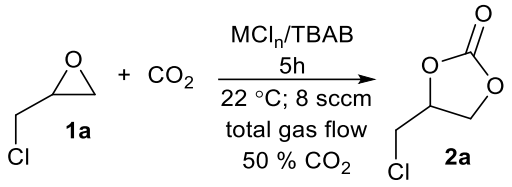

Entry	MCl_n	Conv.(%)[b]	CO_2 conv.(%)[c]	TOF (h^{-1})[d]	$k_{rel}\cdot(10^3)$[e]
1[f]		4	10	0.8	0.6
2[g]		<1			
3	$ZnBr_2$	31	74	6.2	3.8
4	$NbCl_5$	15	36	3	2.0
5	YCl_3	38	91	7.6	4.5
6[h]	YCl_3	33	77	6.6	4.4
7[i]	YCl_3	29	68	5.8	3.3
8	$ScCl_3$	40	95	8	4.7
9	$ZrCl_4$	36	86	7.2	3.8
10	$TaCl_5$	8	19	1.6	1.1
11	$MoCl_5$	0[j]			

[a] Epichlorohydrin 10 mL (11.8 g, 127.5 mmol), catalyst 1.275 mmol (1 mol%), TBAB 2.55 mmol (2 mol%), 5 h, 22 °C with a total flow of 8 sccm (standard cm^3 per minute) using Ar as carrier gas. [b] Conversion determined by ^{1}H-NMR by integration of the corresponding NMR signals of **2a** (4.56 ppm) and of **1a** (2.82 ppm). [c] Calculated on the basis of the amount of CO_2 flowed during the reaction time (1 sccm = $7.43\cdot10^{-7}$ mol·s^{-1}; 53.51 mmol of CO_2 flowed through 300 min) and the conversion of **1a**. [d] Turnover frequency: TON/h; TON: (mmol of product/mmol of metal halide). [e] Apparent initial reaction rate measured from the *in situ* IR profile of formation of **2a**. [f] Under identical conditions as per footnote (a) but without the addition of metal halides. [g] Under identical conditions as per footnote (a) but without the addition of metal halides and using a flow containing 12.5 % CO_2. [h] O_2 was used as carrier gas. [i] Using 2 mol% NEt_4Br (tetraethylammonium bromide) in place of TBAB. [j]The formation of the initial solution led to the rapid formation of polymeric material.

5b. Effect of moisture on the catalytic activity of YCl_3/TBAB

The effect on the reaction of the presence of moisture was investigated by adding increasing amounts of water (in mol % to the epoxide **1a**) to the reaction mixture before flowing gas (50 % CO_2 (v/v) in O_2, in the presence of 1 mol % YCl_3 and 2 mol % TBAB). Following the addition of water, the reaction mixture displayed a gel-like appearance. The apparent initial rates values (k_{rel}) for the formation of **2a** plotted in Figure S4 show that the addition of 0.5 mol % of water (0.5 equiv. to YCl_3) leads already to a drastic reduction of the initial reaction rates, likely due to the formation of a less active Y-species. Consistently, the conversion of **1a** decreases with the amount of water in the initial epoxide solution (See insert in Figure S4). However, carbonate **2a** remained the main reaction product with no increase in the formation of polyepichlorohydrin compared to the reactions carried out with the exclusion of moisture. Remarkably, catalytic activity was observed even in the presence of 25 mol % of water in the mixture. The samples of flue gas employed in this study were found to contain 2 % H_2O (vol.). As for all the other reactions in this study, flue gas was passed through the epoxide solution at a rate of 8 sccm. For a standard catalytic run using epichlorohydrin (127.5 mmol) as substrate, 2400 cm^3 (under STP conditions) of flue gas were passed through the solution in 5 h, corresponding to 48 mL (STP) of water gas. From the ideal gas law it can be calculated that this corresponds to ca. 2 mmol H_2O (ca. 1.6 mol %). Nevertheless, compared to the experiments in Figure S4, this amount of water is added to the solution through the whole reaction period. Moreover, it is unlikely that the entire amount of water in the stream would be absorbed by the solution, but it would be distributed among the gaseous and liquid phase.

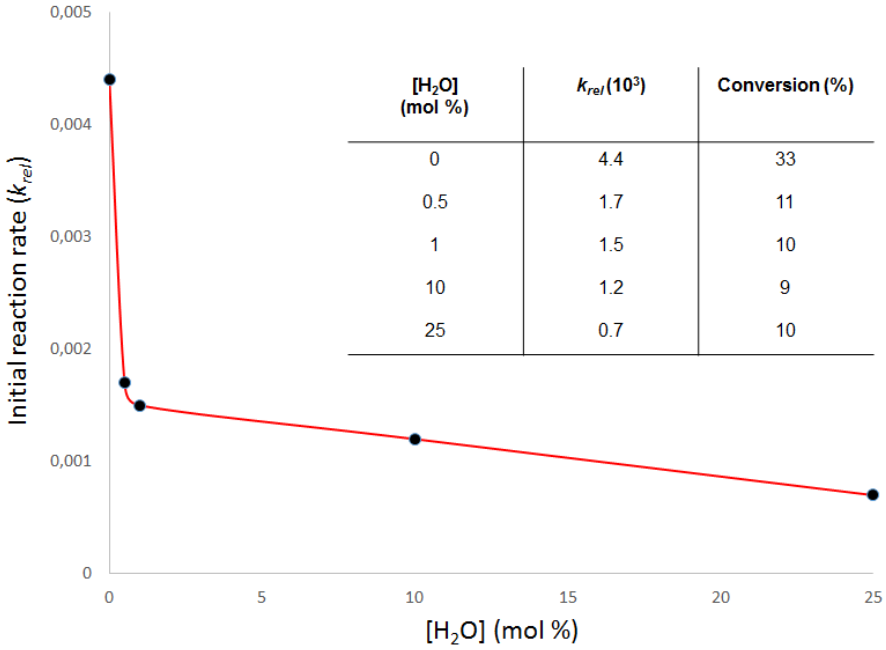

[H_2O] (mol %)	k_{rel}(10^3)	Conversion (%)
0	4.4	33
0.5	1.7	11
1	1.5	10
10	1.2	9
25	0.7	10

Figure S4. Plot of the apparent initial reaction rates for the formation of carbonate **2a** observed by adding increasing amounts of water to a solution of YCl_3 (1 mol %) and TBAB (2 mol %) in epichlorohydrin (127.5 mmol) followed by the exposure to a flow containing 50 % CO_2 (v/v) in O_2; in the insert the conversion of **1a** after 5 h of reaction is reported.

Therefore, it is expected that the presence of 2 % H_2O in the flue gas samples would not strongly affect the reaction kinetics compared to the use of pure flue gases, especially in the initial part of the reaction. This is in a good agreement with the kinetic results presented in Section 6.

6. IR reaction profiles and kinetic studies

The kinetic data and the IR reaction profiles were obtained by monitoring the formation of the carbonate products by *in situ IR*. The method and its application in the study of the kinetics of the cycloaddition of CO_2 to epoxides has been described exhaustively in other reports.[S1-S3] The *in situ IR* profiles for the formation of the carbonate products (IR band at 1810 cm^{-1}) were identical for every reaction in this study and the only differences observed were in the apparent initial rate (slope of the linear segment of the curve at 1810 cm^{-1}) and in the degree of conversion reached after 5 h (final value of the absorption). The formation of the carbonate product was preceded by the formation of a signal at about 1660 cm^{-1} attributable to the hemicarbonate intermediate.[29a] This observation corresponded to an induction time of 20-30 min for the formation of the product (See for instance Figures S5, S6). The i*n situ* IR profiles for the reactions carried out using samples of flue gas were comparable to those obtained for the reactions with mixtures of pure gases (See Figure S7 for epoxide **1a** and flue gas and Figure S8 for epoxide **1b** and flue gas).

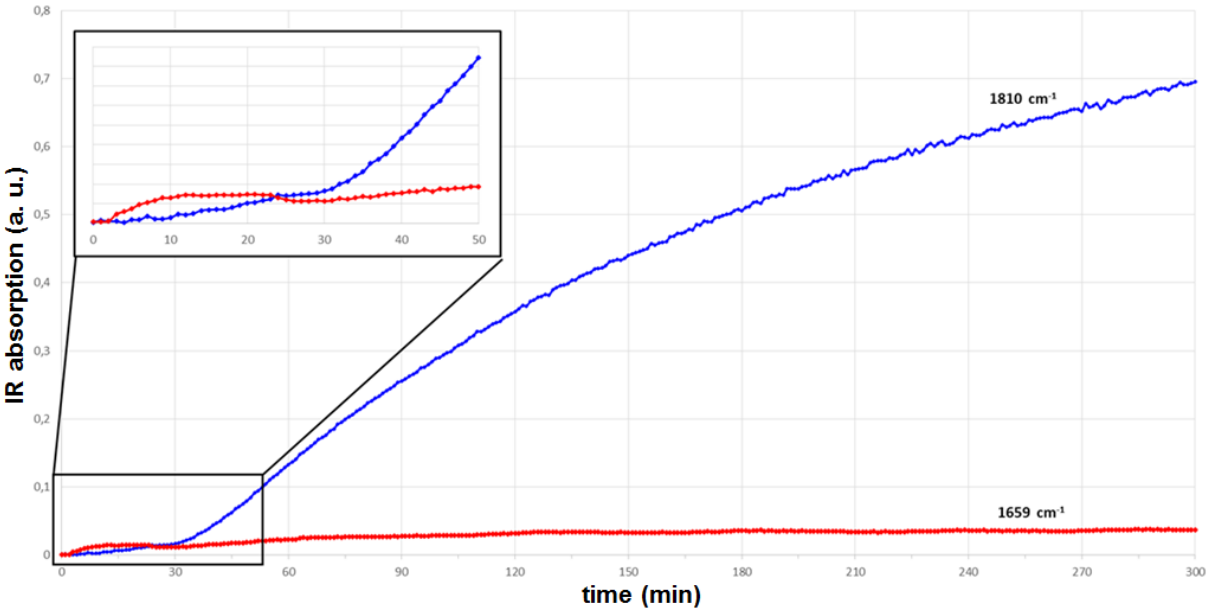

Figure S5. *In situ* IR profile for the formation of carbonate **2a** ($\nu_{C=O}$ = 1810 cm^{-1}) from CO_2 and **1a** (50 % CO_2 v/v, 23 °C, total flow 8 sccm, carrier gas O_2, 5 h) showing an induction time due to the formation of the hemicarbonate species at 1659 cm^{-1}.

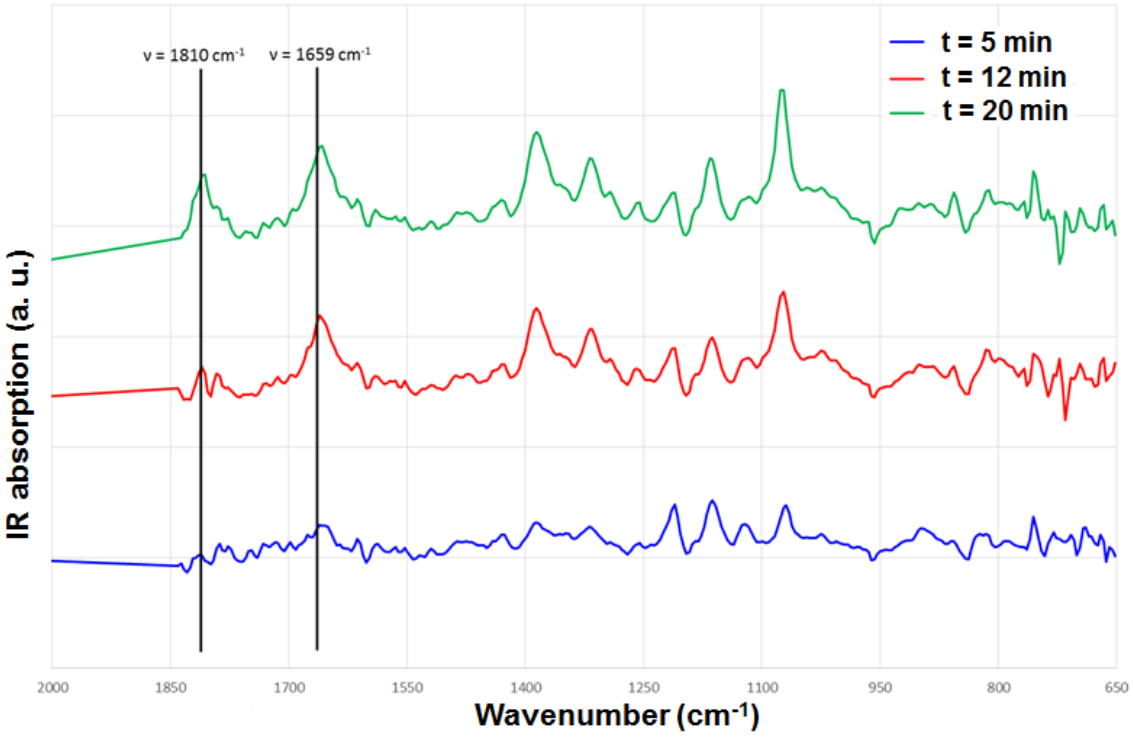

Figure S6. *In situ* IR spectra of the reaction in Figure S5 taken at three different stages of the induction period and showing the formation of the hemicarbonate intermediate ($\nu_{C=O}$ = 1659 cm^{-1}) before of the formation of carbonate **2a** ($\nu_{C=O}$ = 1810 cm^{-1}).

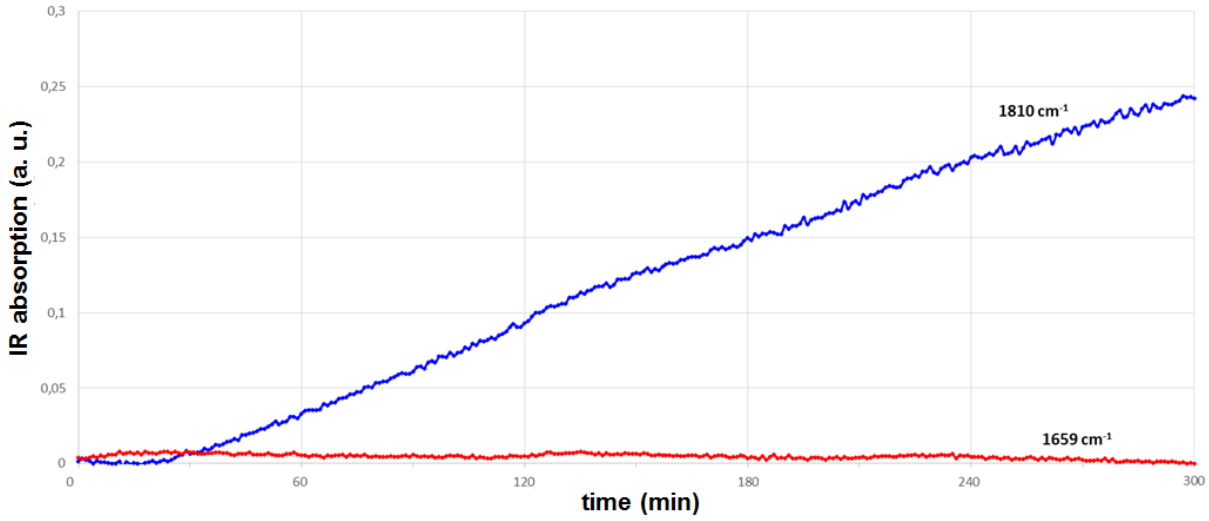

Figure S7. *In situ* IR profile for the formation of carbonate **2a** ($\nu_{C=O}$ = 1810 cm^{-1}) from flue gas CO_2 and **1a** (10.2 % CO_2 v/v, 23 °C, total flow 8 sccm, 5 h).

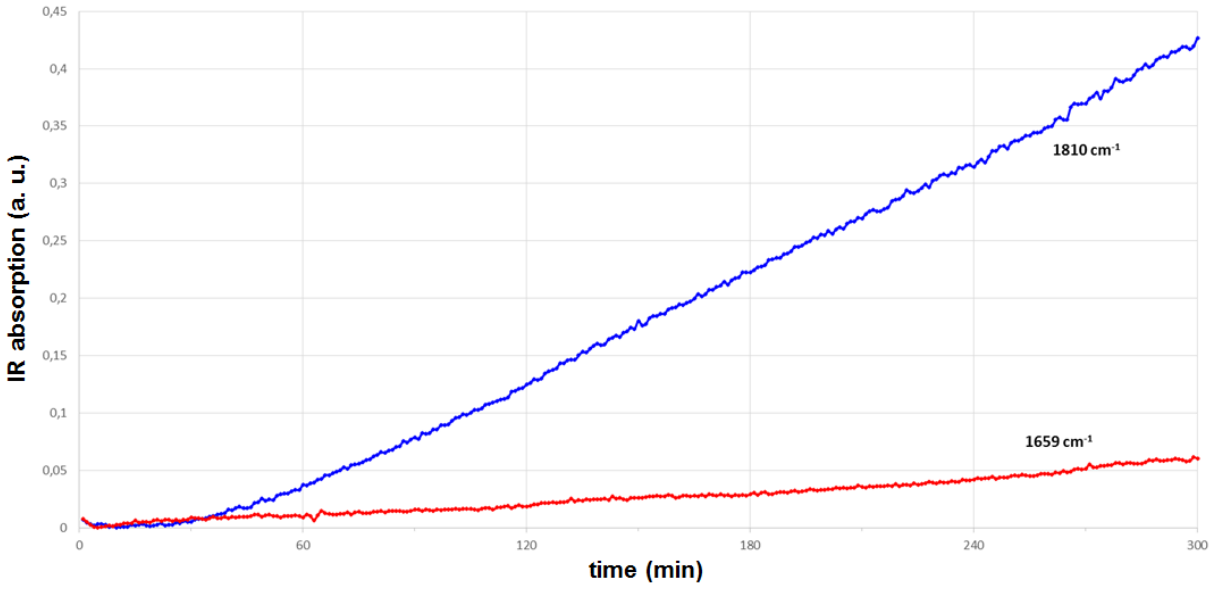

Figure S8. *In situ* IR profile for the formation of carbonate **2b** ($\nu_{C=O}$ = 1810 cm^{-1}) from flue gas CO_2 and **1b** (10.2 % CO_2 v/v, 23 °C, total flow 8 sccm, 5 h).

We used the apparent initial rate of formation of **2a** (k_{rel}) at different [CO_2] in the slipstream to determine the reaction order of CO_2 (considering that the [CO_2] in the epoxide solution would be proportional to that in the gas flow) and to analyze the behavior of flue gas as an impure CO_2 source. The values of k_{rel} determined for various [CO_2] values (including the reaction with flue gas) for the reaction of **1a** and CO_2 catalyzed by YCl_3 and TBAB under otherwise identical conditions are presented in Table S4. The plot of k_{rel} versus [CO_2] is reported in Figure S9.

Table S4: Apparent initial reaction rate values (k_{rel}) for the cycloaddition of CO_2 to epoxide **1a** catalyzed by YCl_3 (1 mol %) and TBAB (2 mol %) at various [CO_2].

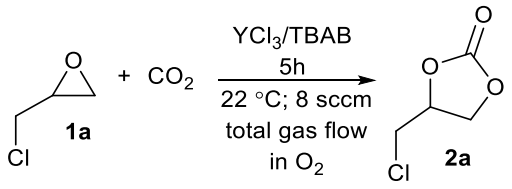

Entry	[CO_2] (%)	$k_{rel}\cdot(10^3)$
1[a]	10.2	0.9
2	12.5	1.1
3	25	1.9
4	50	4.4
5	75	6.6
6	100	6.9

[a] Values relative to the use of flue gas samples.

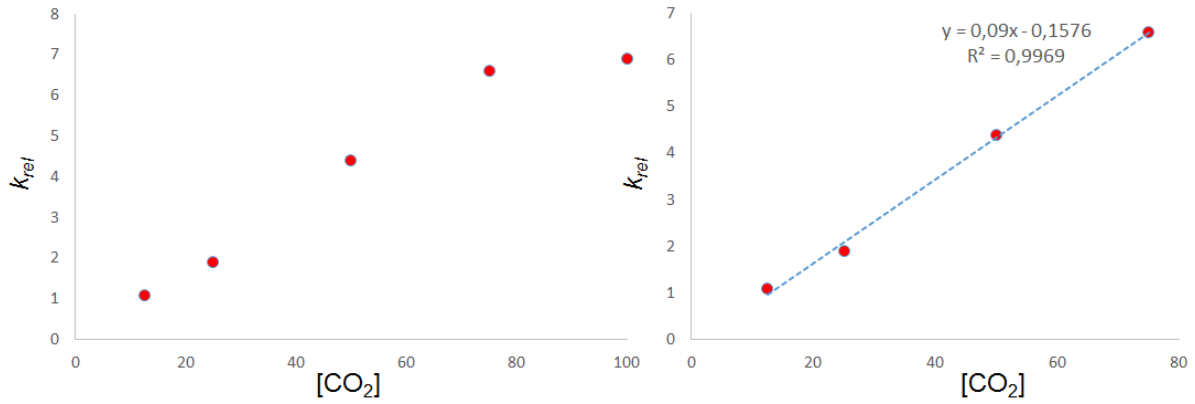

Figure S9. (Left) Dependency of k_{rel} on [CO_2] for the runs employing a stream of pure gases as a diluted CO_2 source; (Right) with the exclusion of the run with [CO_2] = 100 %, the values of k_{rel} versus [CO_2] display a linear correlation.

By initially considering only the runs employing mixtures of pure gases, a linear correlation was observed between k_{rel} and [CO_2] with the exclusion of the catalytic run employing pure CO_2 ([CO_2] = 100 %). This can be attributed to a saturation effect of the epoxide solution for values of [CO_2] in the gas flow lower than 100 % (likely 75-80 %).

When the reaction carried out using a sample of flue gas as a CO_2 source was taken into account amongst the catalytic runs in Figure S9 (Right, [CO_2] ≤ 75 %), we did not notice any significant deviation from the trend defined by the reactions carried out by employing mixtures of pure CO_2 in O_2 (Figure S10, Left). The double logarithmic plot of $Log_{10}(k_{rel})$ versus Log_{10}[CO_2] shows once again a linear trend with a slope of 1. This indicates a first order dependency of the reaction rate on [CO_2] (Figure S10, Right).

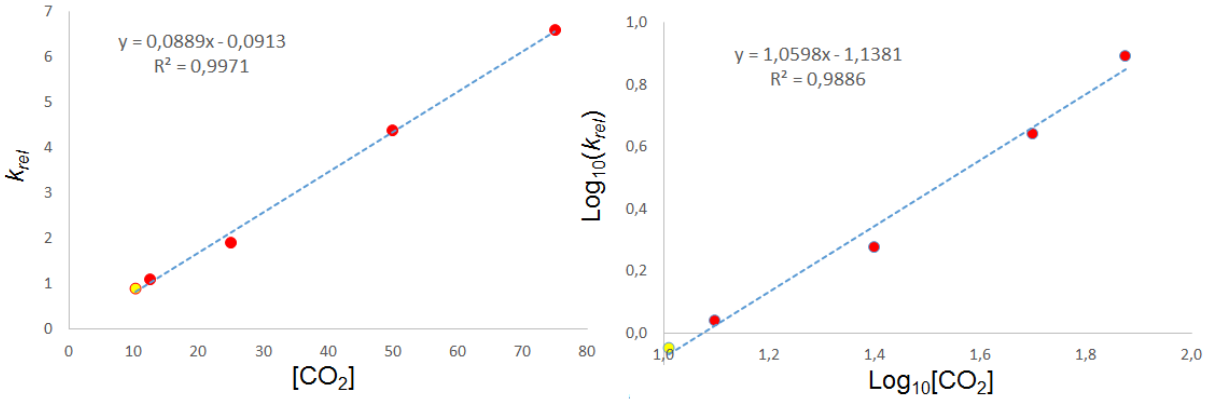

Figure S10. (Left) Dependency of k_{rel} on [CO_2] for all the reactions in Table S4 ([CO_2] ≤ 75 %) including the test with flue gas (Table S4, Entry 1, yellow marker); (Right) double logarithmic plot of $Log_{10}(k_{rel})$ versus Log_{10}[CO_2] showing a linear trend with a slope of ca. 1.

7. NMR spectra of the products of the catalytic runs

The ^{1}H NMR ($CDCl_3$) of a typical catalysis run using YCl_3 as a catalyst and **1a** as substrate (50 % CO_2; 1 mol % YCl_3; 2 mol % TBAB, r.t., 5 h, gas carrier O_2) is displayed in Figure S11:

Assignment of the ^{1}H NMR shifts:

(*) TBAB: 3.40 (8H, it was often found to coalesce with the signal of **1a** at 3.17 ppm), 1.59 (8H), 1.37 (8H), 0.94 (12H) ppm; see also Ref. S4 below.

(&) 1a: 3.57 and 3.47 (2H, ClC*H*$_2$CH), 3.17 (1H, ClCH$_2$C*H*), 2.83 (1H, CHC*H*$_A$H$_B$), 2.63 (1H, CHCH$_A$*H*$_B$) ppm; see also Ref. S5 below.

(#) 2a: 4.97 (1H, ClCH$_2$C*H*), 4.56 (1H, CHC*H*$_A$H$_B$), 4.36 (1H, CHCH$_A$*H*$_B$), 3.76 and 3.72 (2H, ClC*H*$_2$CH), see also Ref. 34

Additionally, all the spectra of the reactions carried out using **1a** as a substrate present additional signals at 4.02 and 3.64 ppm (marked with **x** in Figure S11). The ratio between the integral of these signals (integral of the signal at 3.64 ppm/integral of the signal at 4.02 ppm) is in always in the 4:1 to 7:1 range but the signal at 3.64 ppm partially overlaps with the ClC*H*$_2$CH signals of **1a** and **2a**.

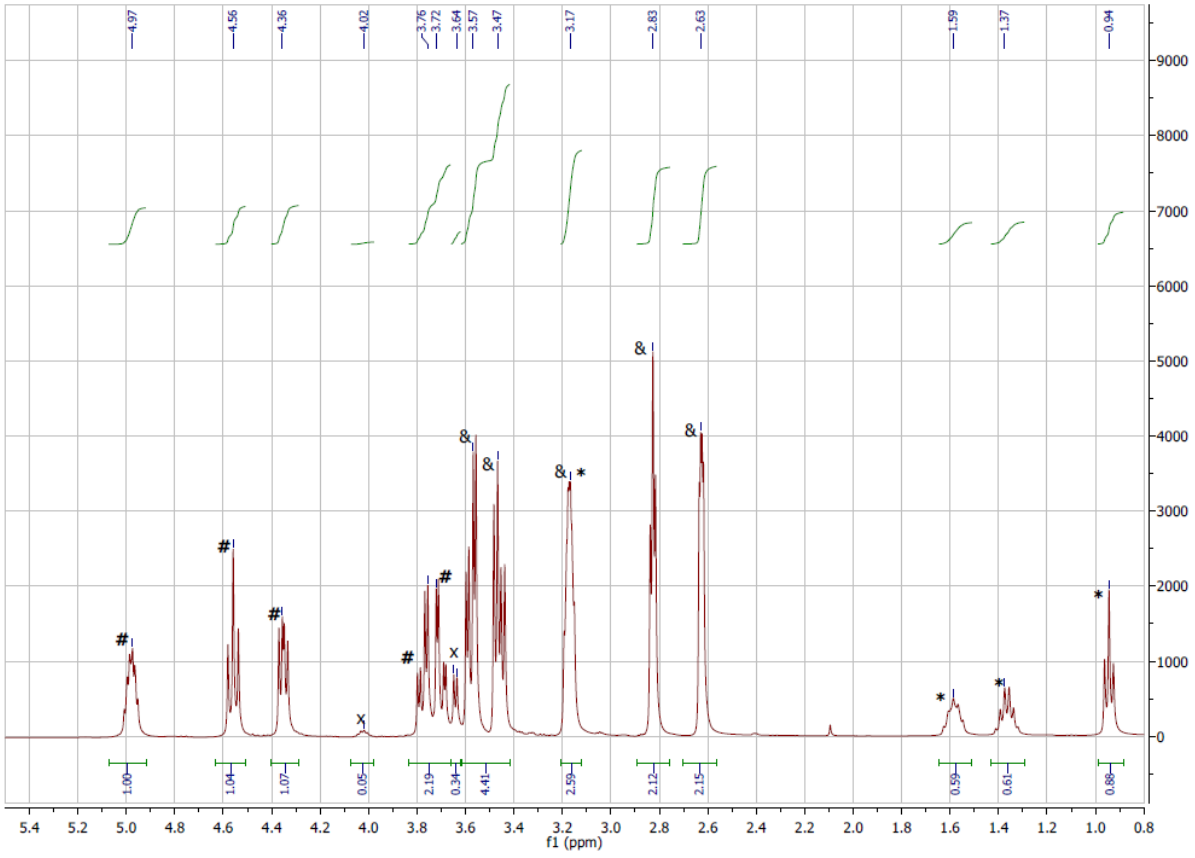

Figure S11. ^{1}H NMR spectrum of a typical catalytic run using **1a** as substrate (50 % CO_2; 1 mol % YCl_3; 2 mol % TBAB, r.t., 5 h, gas carrier O_2). All shifts are assigned.

According to the literature, the signal at 3.64 ppm could be attributed to the formation of polyepichlorohydrin that is reported as a broad signal in the 3.89-3.49 ppm region (5H).[40] Nevertheless, this signal could also be attributed to the metal-alcoholate formed upon opening of epoxide **1a** (See intermediate **I** in Scheme 1). This intermediate is supposed to be present in solution at the end of the reaction as the epoxide substrate is used in excess. In order to gain deeper insight, in an NMR experiment equimolar amounts of YCl_3, TBAB and **1a** (0.15 mmol) were allowed to react for 5 h in 1 mL of $CDCl_3$. Upon the nearly complete dissolution of YCl_3 an aliquot of the solution was withdrawn and analyzed by ^{1} H NMR. The solution appeared clear with no apparent trace of polymers. The complete absence of signals in the 2.5-3.3 ppm region confirmed the complete conversion of **1a** (Figure S12). Along with the signals relative to the tetrabutylammonium salt, two new signals appeared at 3.68 ppm (4H) and at 4.11 ppm (1H). These signal are in good agreement with those observed in the NMR of the reaction mixture and could be attributed to the 5H of the metal alcoholate intermediate. To note, an analogous alcoholate of $NbCl_5$ with propylene oxide has been reported and its protons were found to have ^{1}H NMR chemical shifts of 4.23, 3.92 and 3.40 ppm.[29a] Based on these observations, it is likely that the signals found at 3.64 and 4.02 ppm should be attributed to the presence of the metal alcoholate rather than polyepichlorohydrin. The observation that this signal is more evident (compared to that of **2a**) for those reactions that gave a lower yield of **2a** corroborates this hypothesis as the concentration of the catalyst (and therefore of the alcoholate) was kept constant through all the catalytic runs. In the ^{1}H NMR spectra of the metal halides that afforded a lower yield of the carbonate products ($TaCl_5$; $NbCl_5$) an additional broad signal at 4.67 ppm is observed. As these spectra were measured after exposure of the reaction mixture to air it is likely that this signal arises from the reaction of the alcoholates with moisture leading to the formation of –OH moieties.

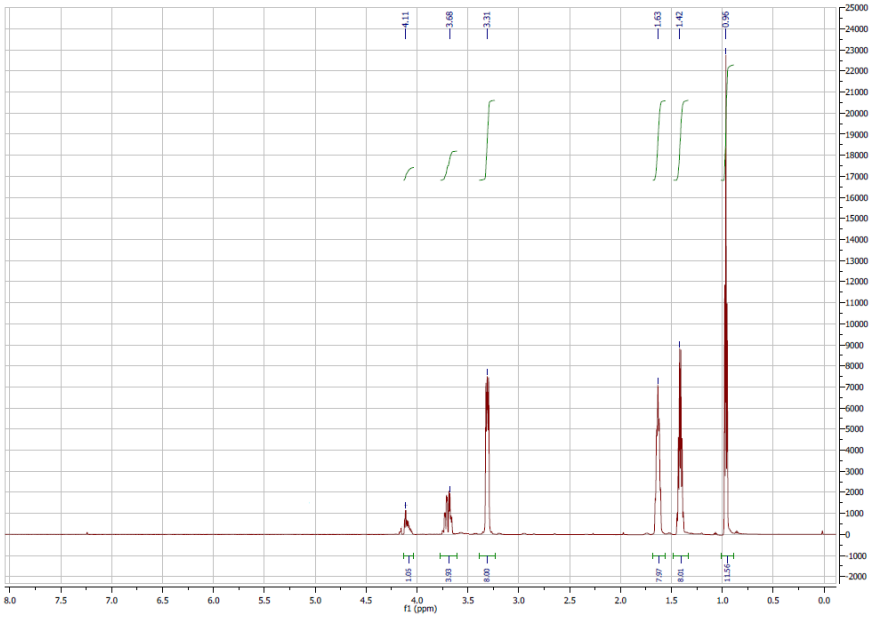

Figure S12. ^{1}H NMR spectrum of an equimolar mixture of **1a**, TBAB and YCl_3 allowed to stir for 5 h in $CDCl_3$.

Chart 1, Entry 2 (Table S3, Entry 1) epoxide **1a**, 50 % CO_2 in Ar, 5 h, Catalyst: TBAB

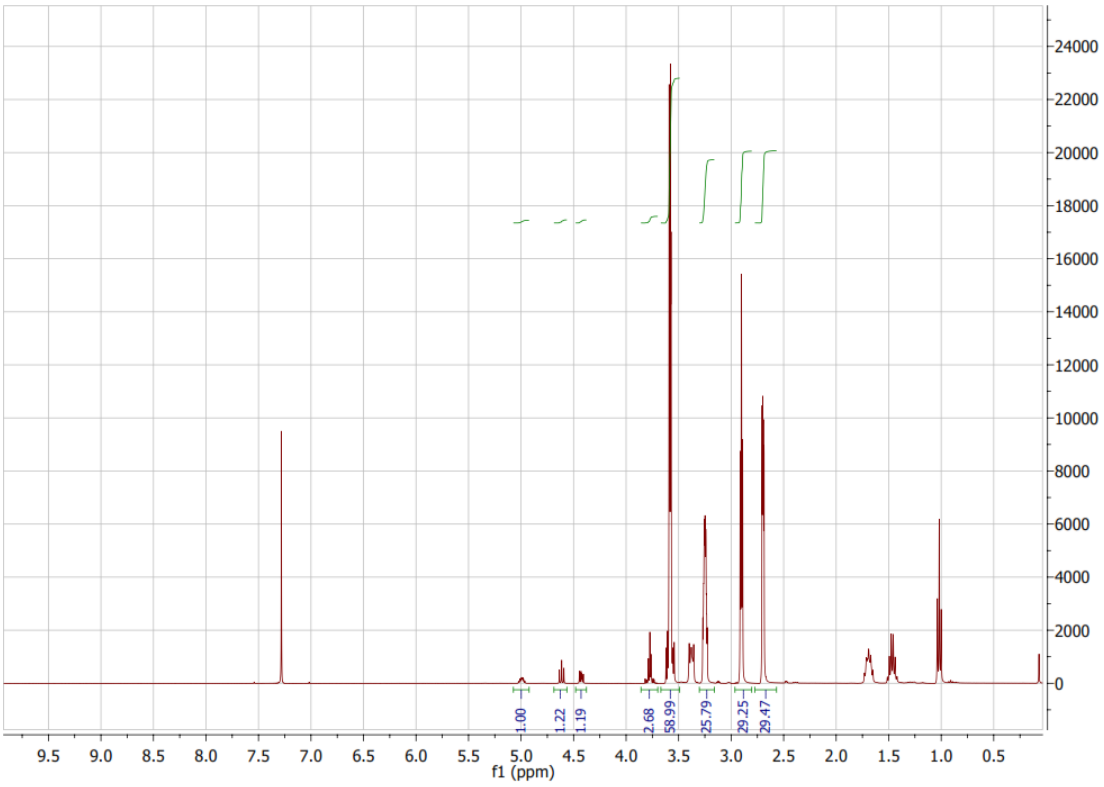

Chart 1, Entry 3 (Table S3, Entry 7) epoxide **1a**, 50 % CO_2 in Ar, 5 h, Catalyst: $TaCl_5$/TBAB

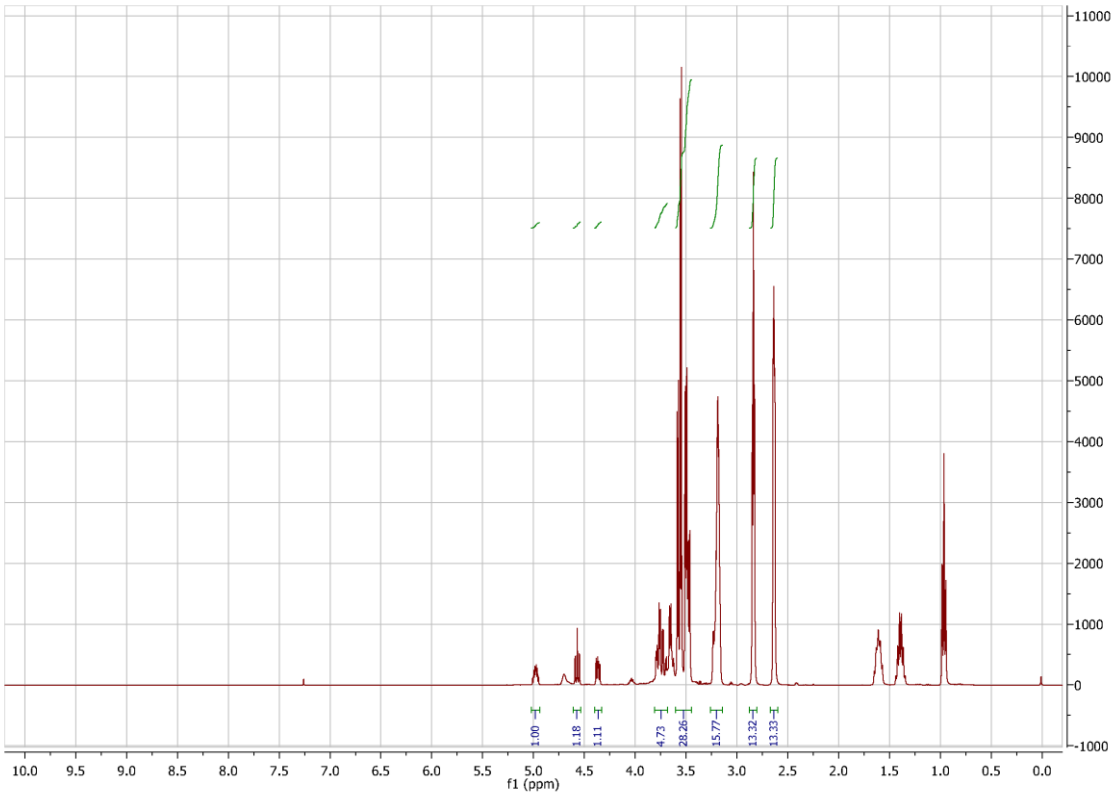

Chart 1, Entry 4 (Table S3, Entry 4) epoxide **1a**, 50 % CO_2 in Ar, 5 h, Catalyst: $NbCl_5$/TBAB

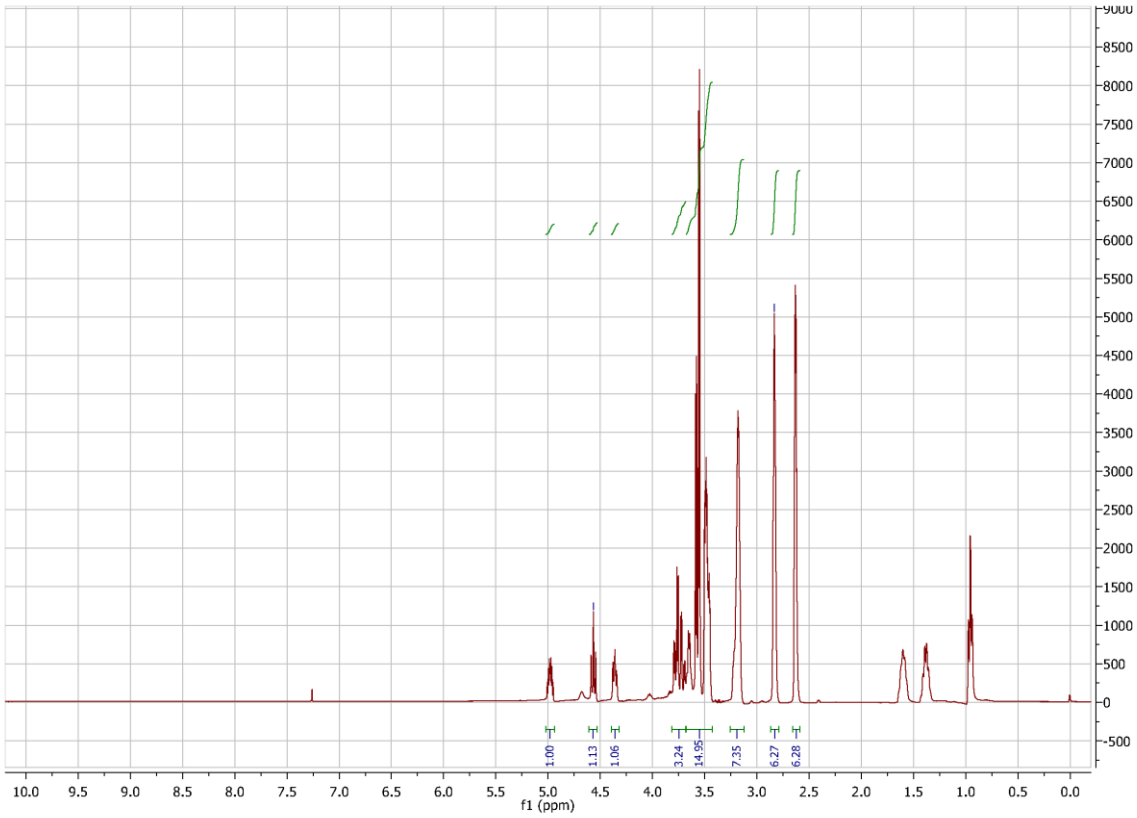

Chart 1, Entry 5 (Table S3, Entry 4) epoxide **1a**, 50 % CO_2 in O_2, 5 h, Catalyst: YCl_3/TBAB

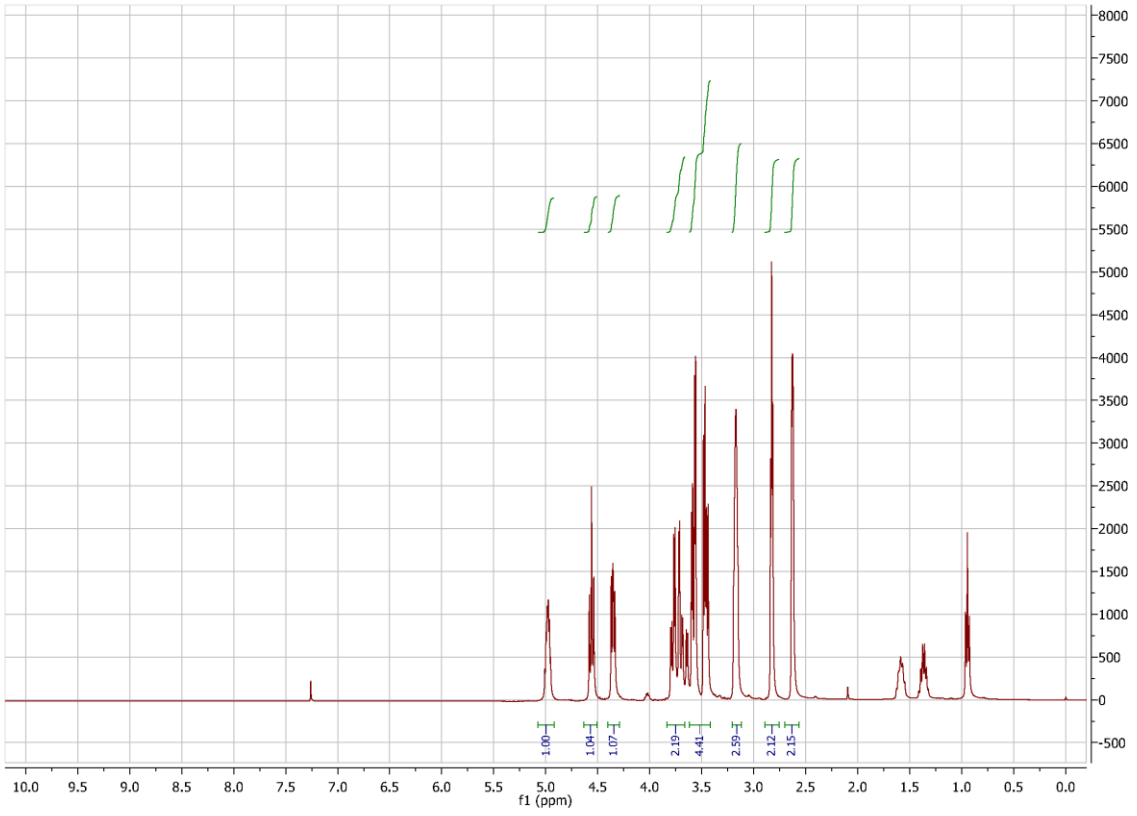

Chart 1, Entry 6 (Table S3, Entry 6) epoxide **1a**, 50 % CO_2 in Ar, 5 h, Catalyst: $ZrCl_4$/TBAB

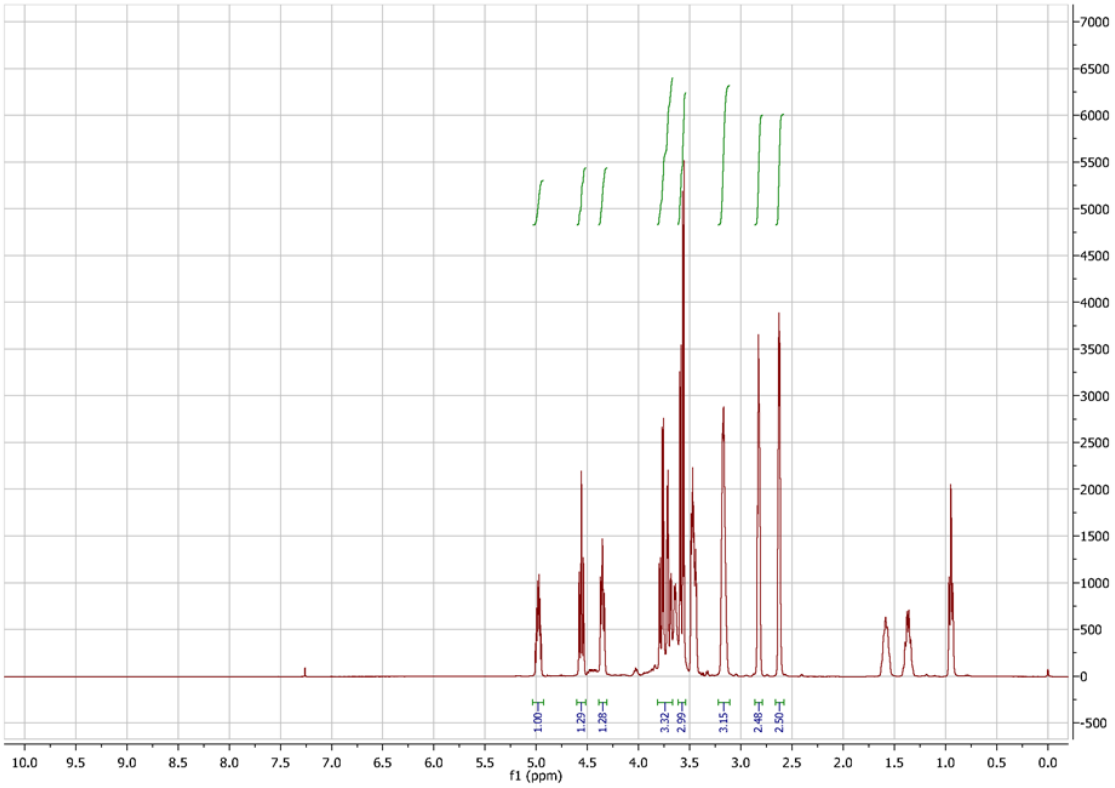

Chart 1, Entry 7 (Table S3, Entry 3) epoxide **1a**, 50 % CO_2 in Ar, 5 h, Catalyst: YCl_3/TBAB

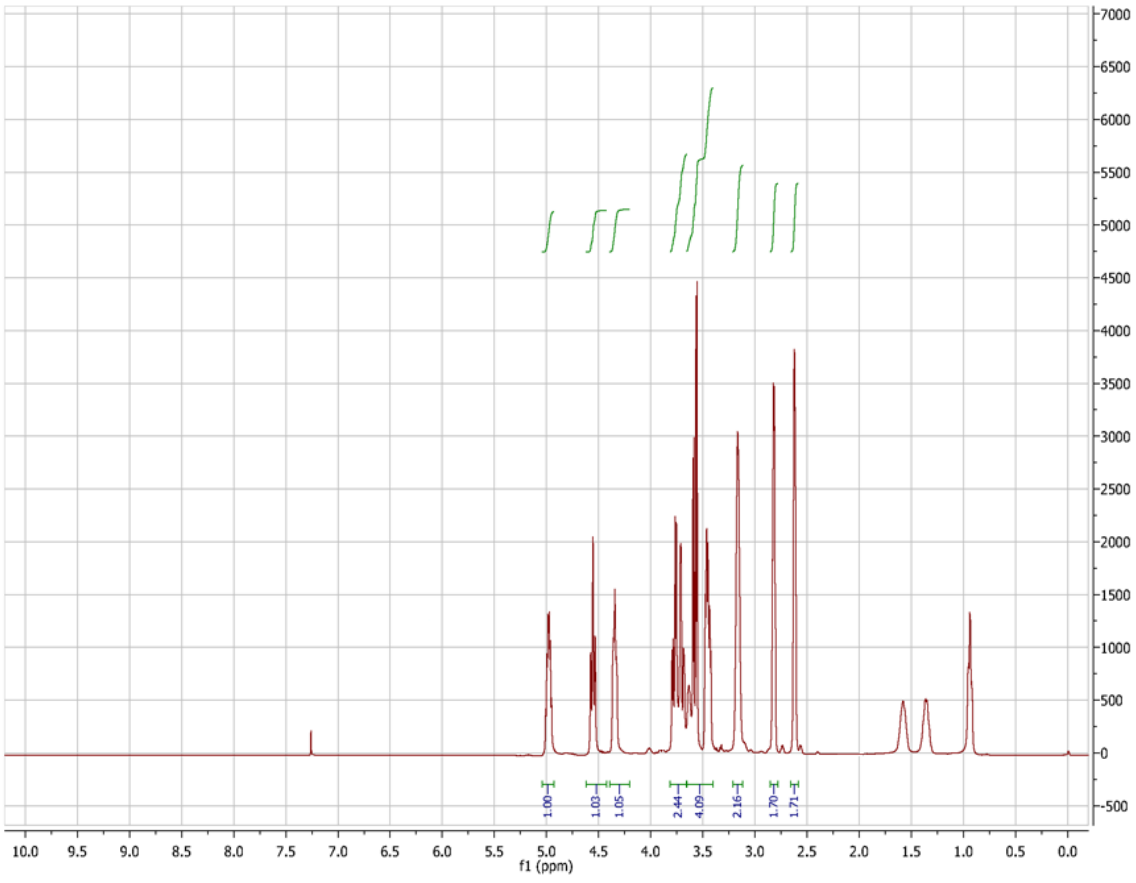

Chart 1, Entry 8 (Table S3, Entry 5) epoxide **1a**, 50 % CO_2 in Ar, 5 h, Catalyst: $ScCl_3$/TBAB

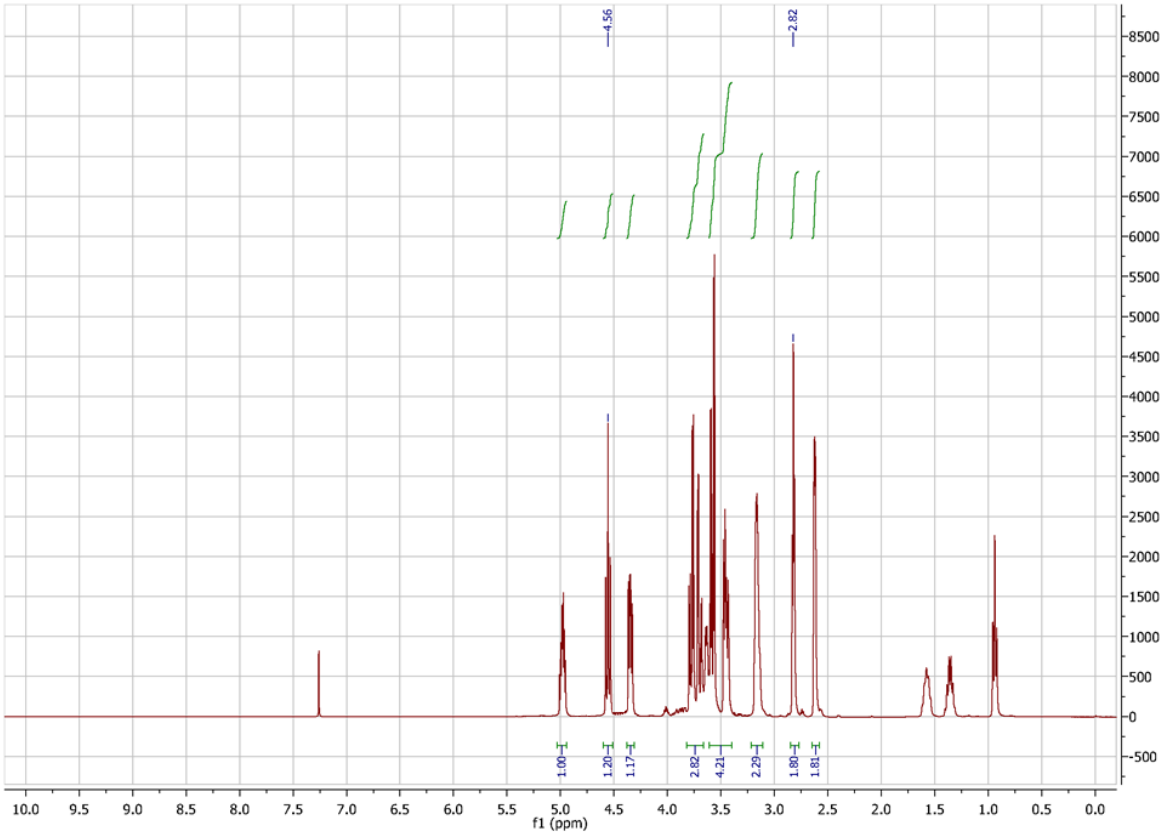

Table 1, Entry 2 epoxide **1b**, 50 % CO_2 in O_2, 5 h, Catalyst: YCl_3/TBAB

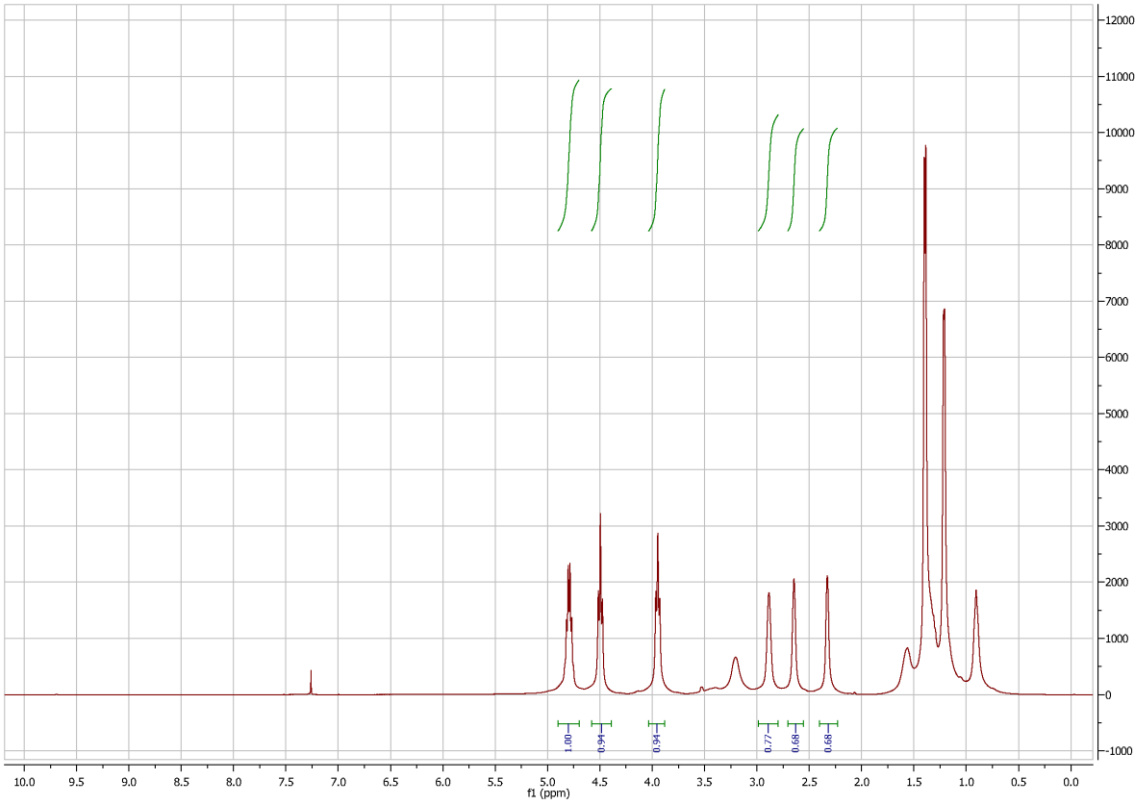

Table 1, Entry 3 epoxide **1b**, 50 % CO_2 in O_2, 5 h, Catalyst: YCl_3/TBAB (At 0 °C)

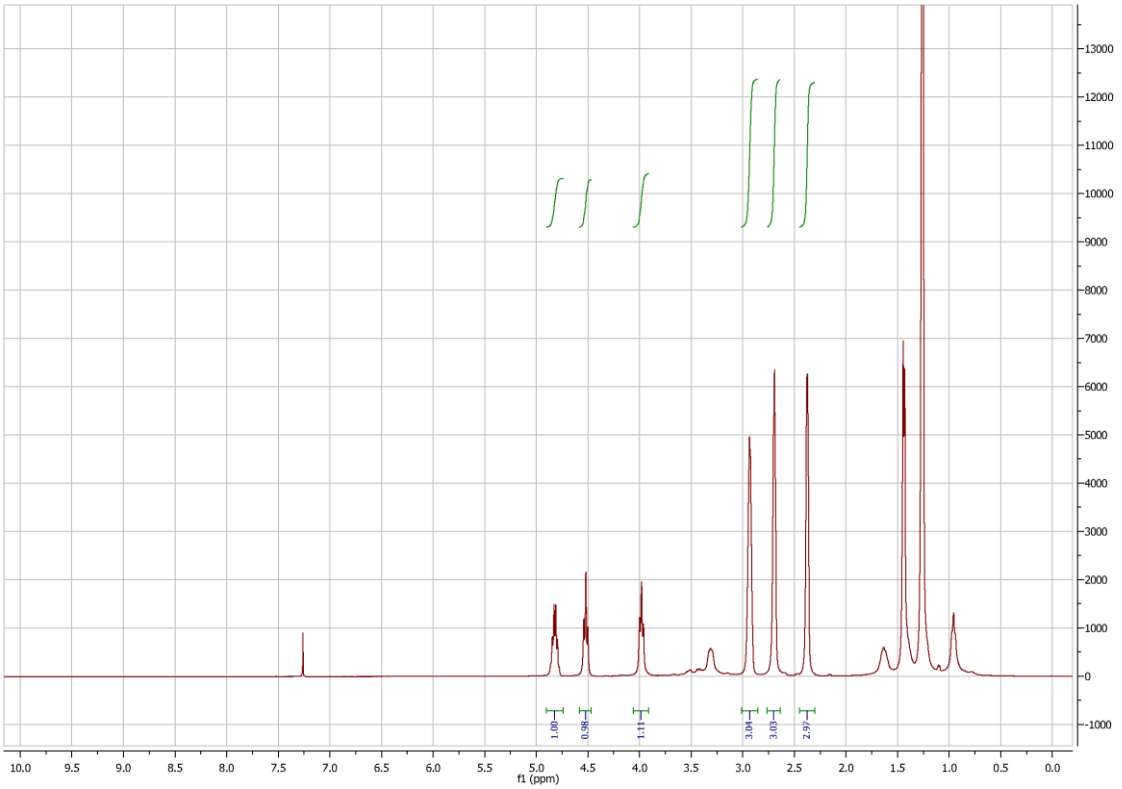

Table 1, Entry 4 epoxide **1c**, 50 % CO_2 in O_2, 5 h, Catalyst: YCl_3/TBAB

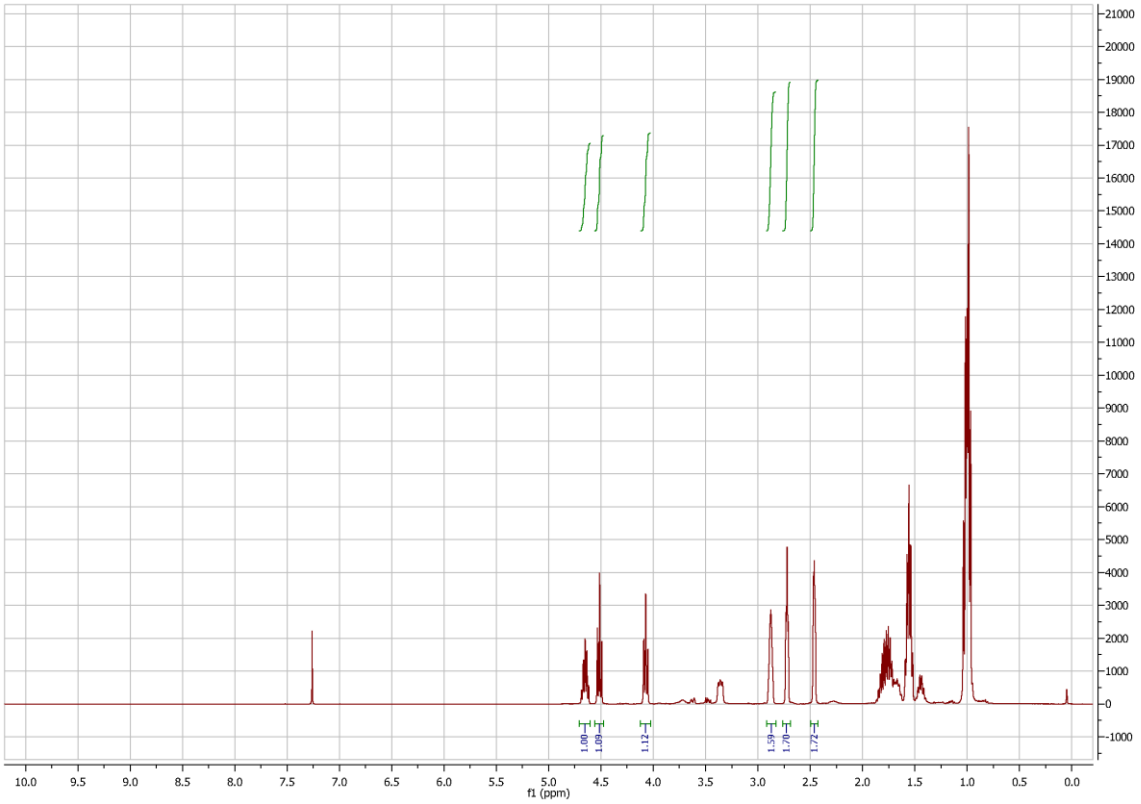

Table 1, Entry 5 epoxide **1d**, 50 % CO_2 in O_2, 5 h, Catalyst: YCl_3/TBAB

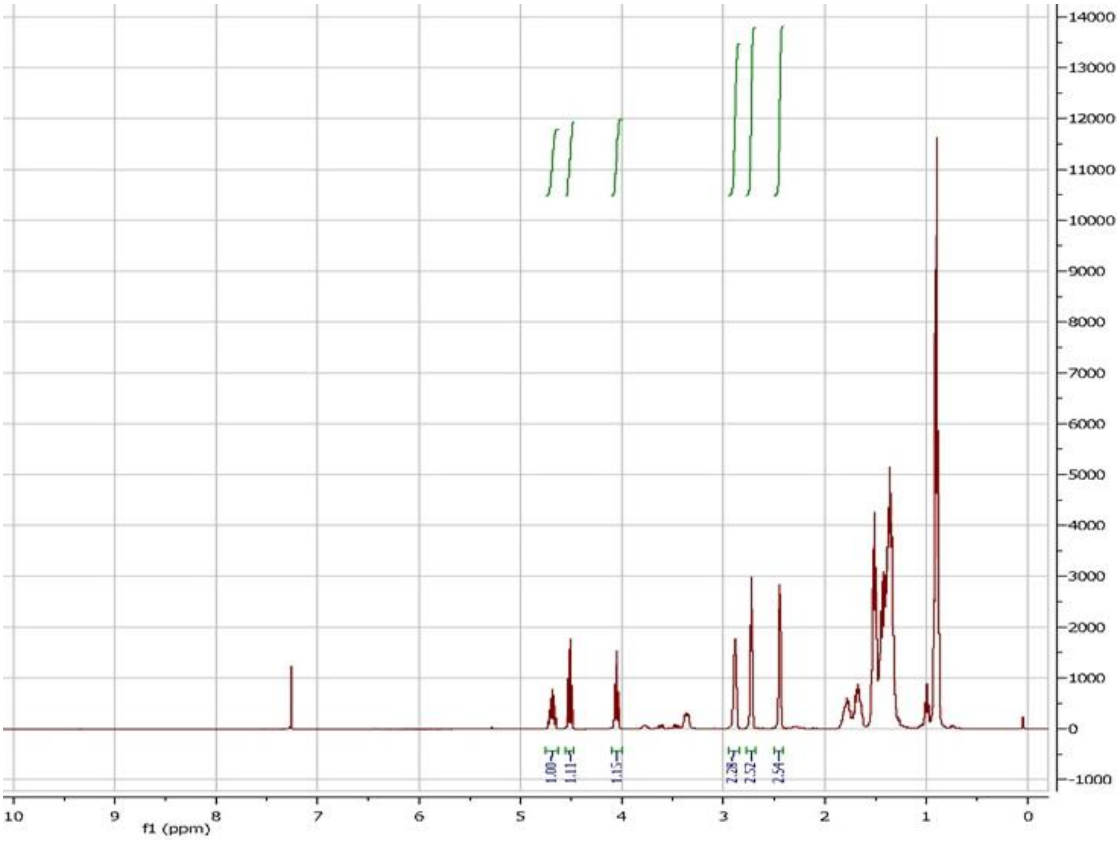

Table 1, Entry 6 epoxide **1e**, 50 % CO_2 in O_2, 5 h, Catalyst: YCl_3/TBAB

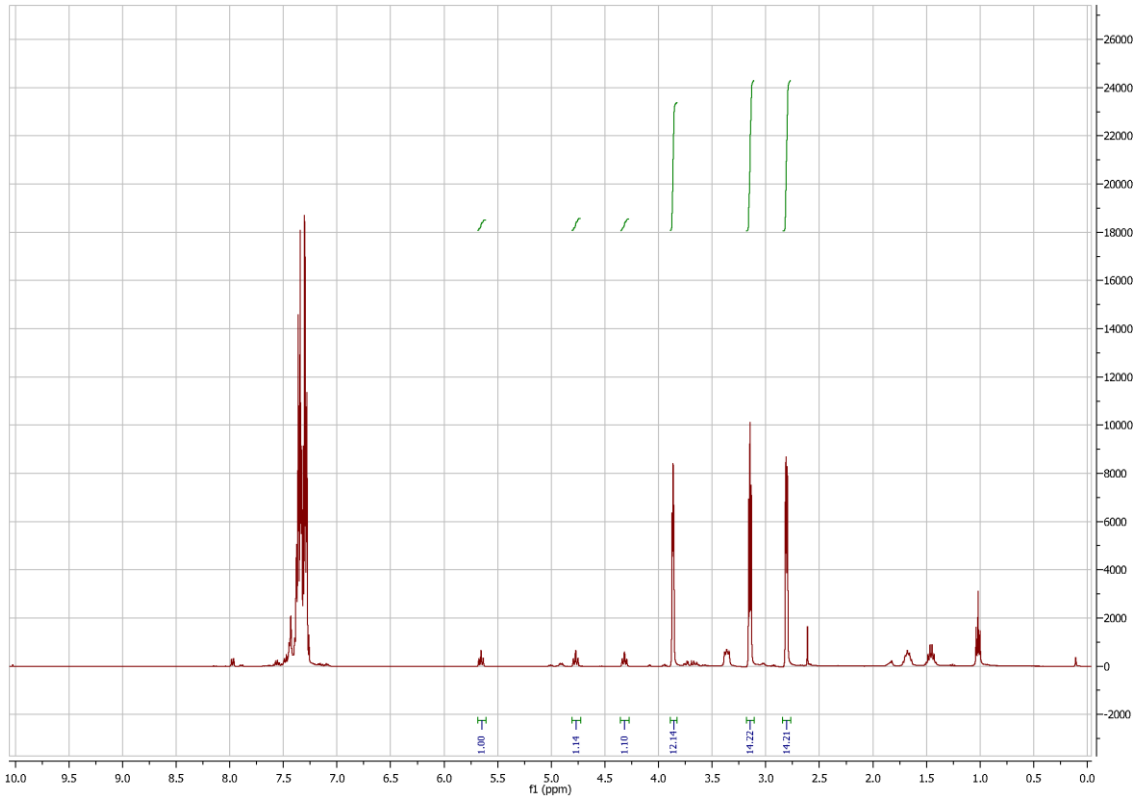

Table 2, Entry 1 epoxide **1a**, 100 % CO_2, 5 h, Catalyst: YCl_3/TBAB

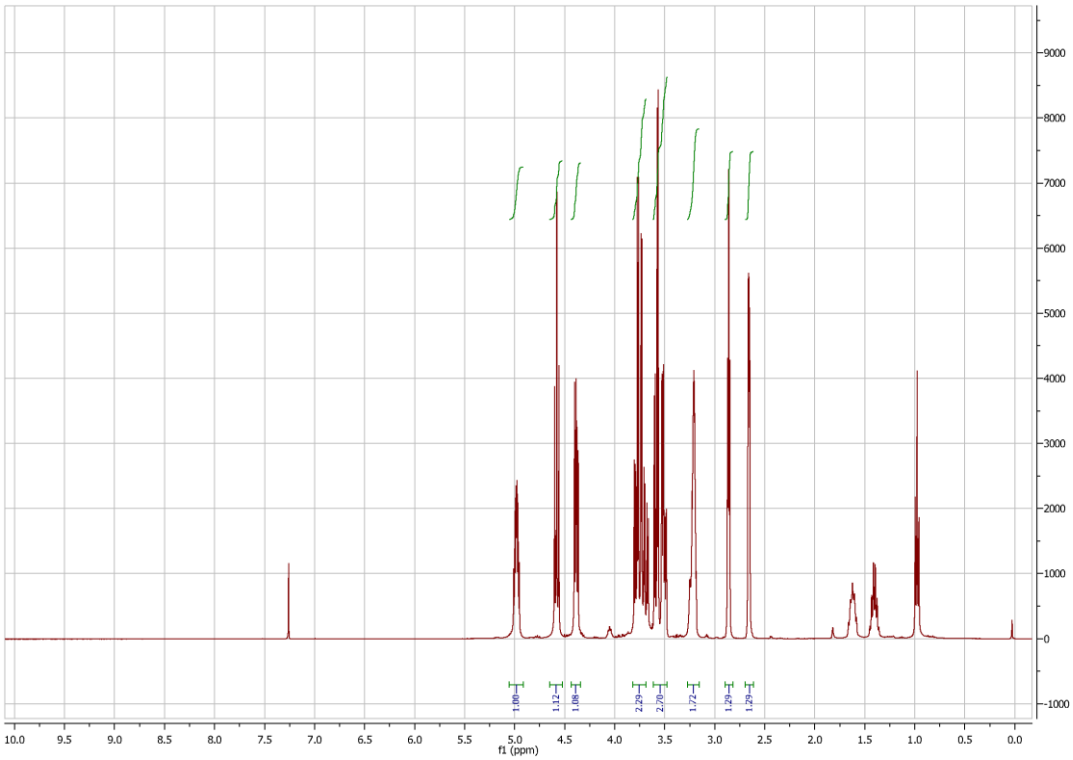

Table 2, Entry 2 epoxide **1a**, 100 % CO_2, 3 h, Catalyst: YCl_3/TBAB

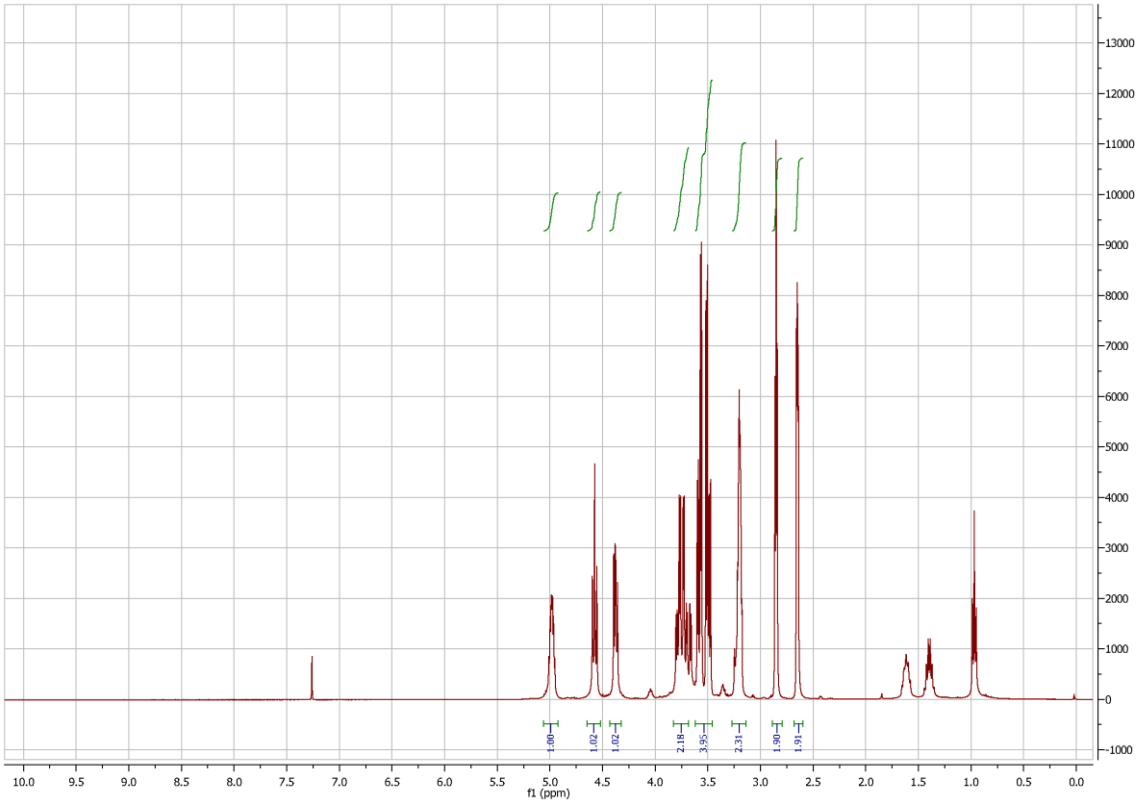

Table 2, Entry 3 epoxide **1a**, 75 % CO_2 in O_2, 5 h, Catalyst: YCl_3/TBAB

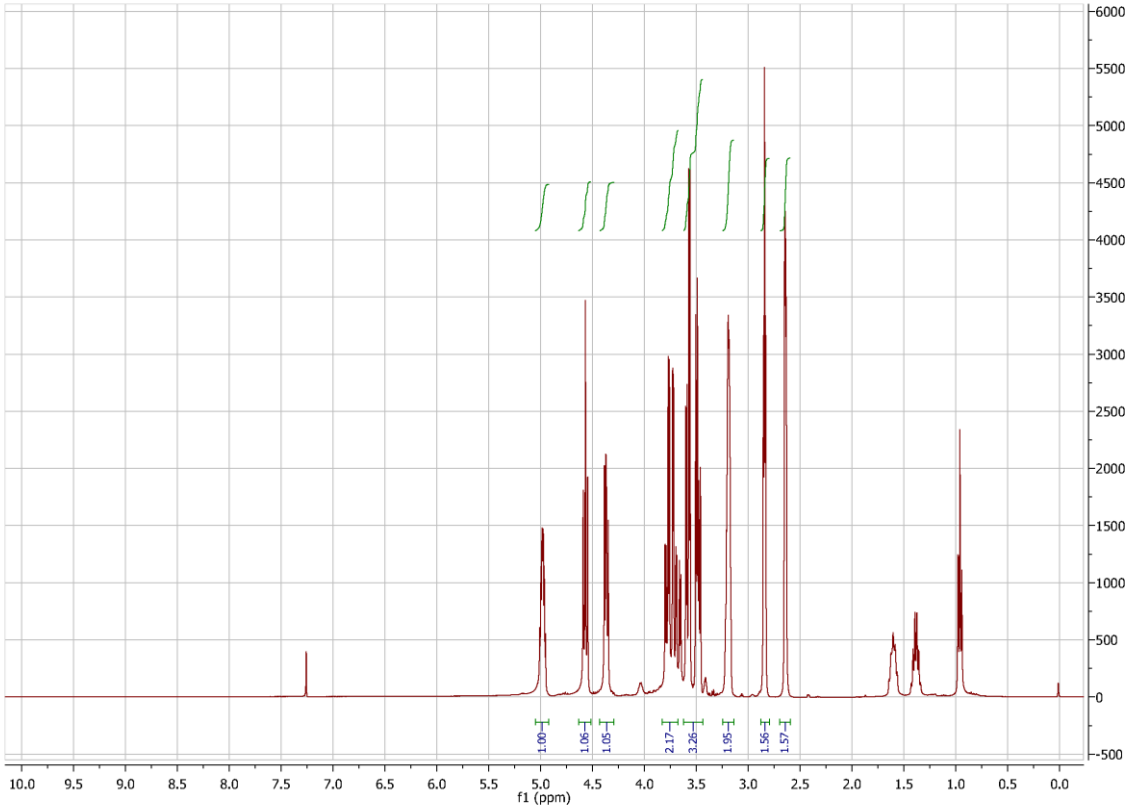

Table 2, Entry 4 epoxide **1a**, 50 % CO_2 in O_2, 5 h, Catalyst: YCl_3/TBAB

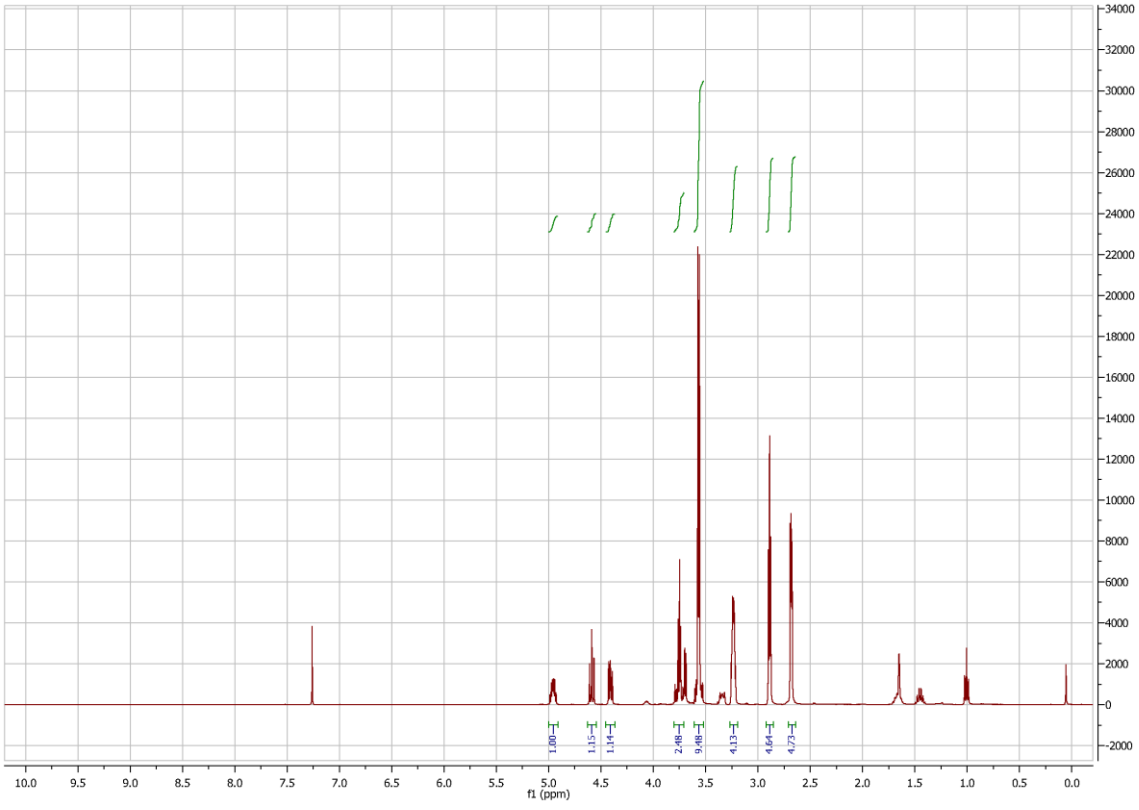

Table 2, Entry 5 epoxide **1a**, 50 % CO_2 in O_2, 5 h, Catalyst: YCl_3/TBAB (1 mol % TBAB)

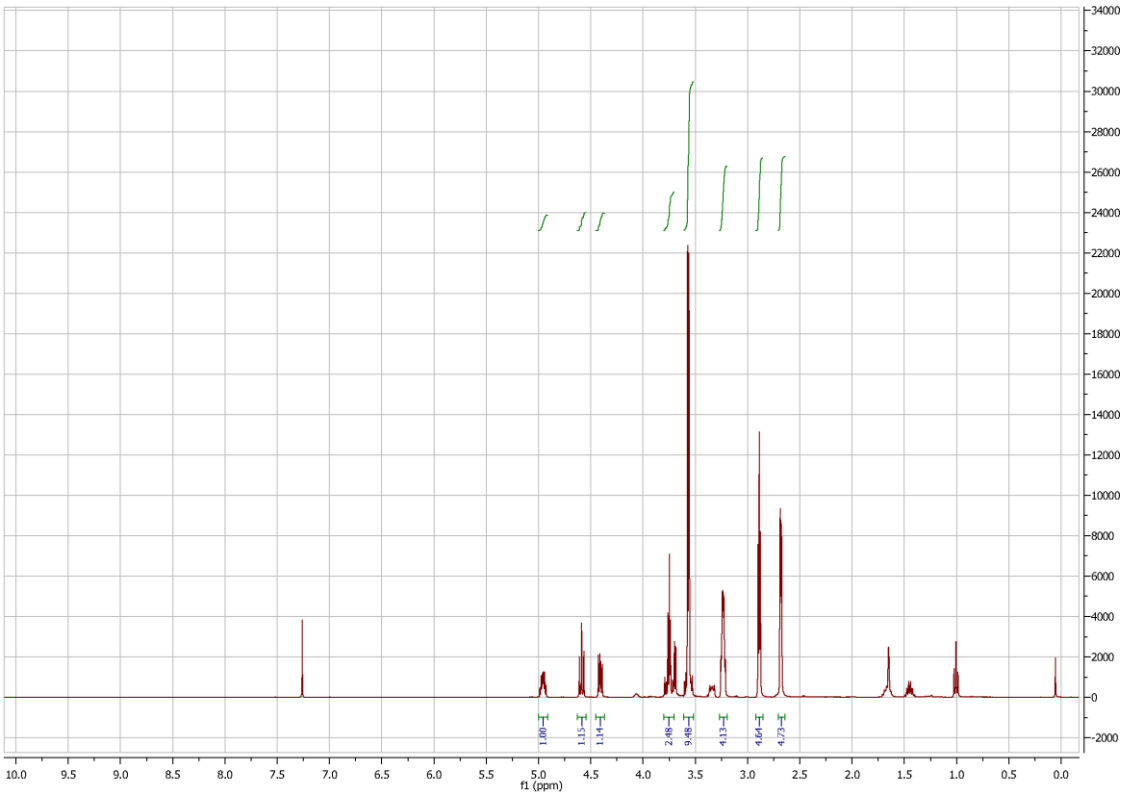

Table 2, Entry 6 epoxide **1a**, 50 % CO_2 in O_2, 3 h, Catalyst: YCl_3/TBAB

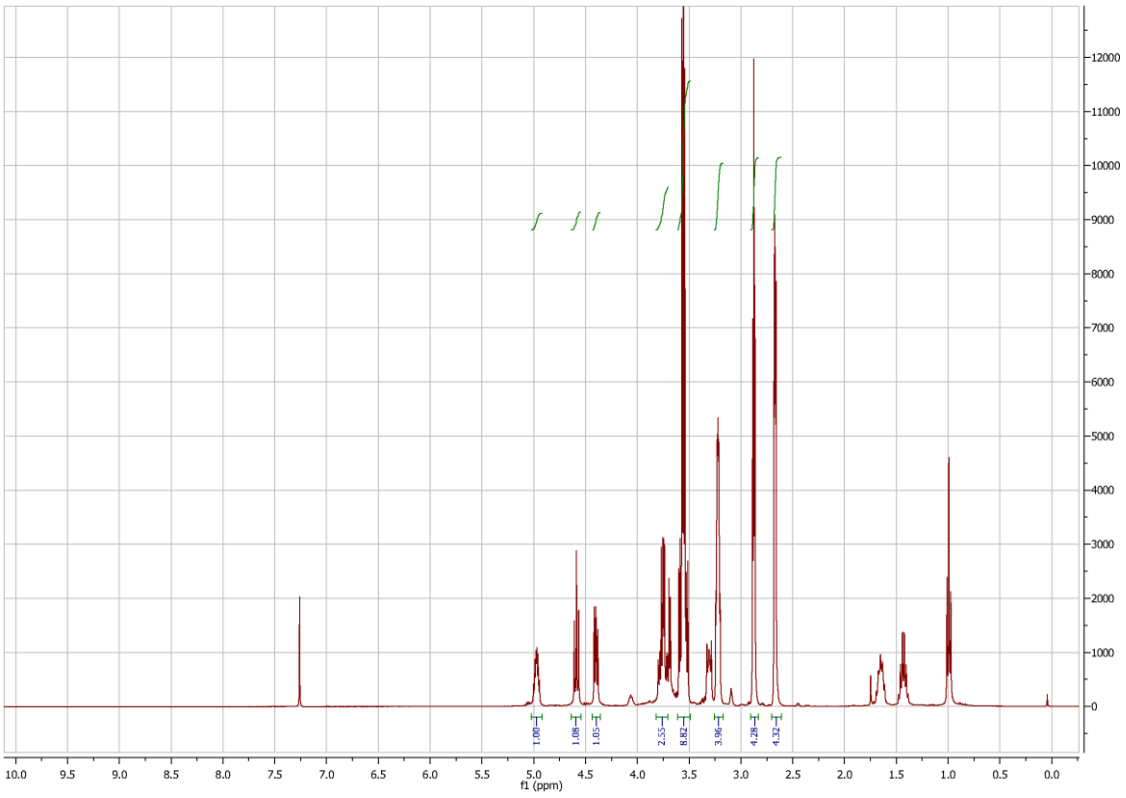

Table 2, Entry 7 epoxide **1a**, 50 % CO_2 in O_2, 24 h, Catalyst: YCl_3/TBAB

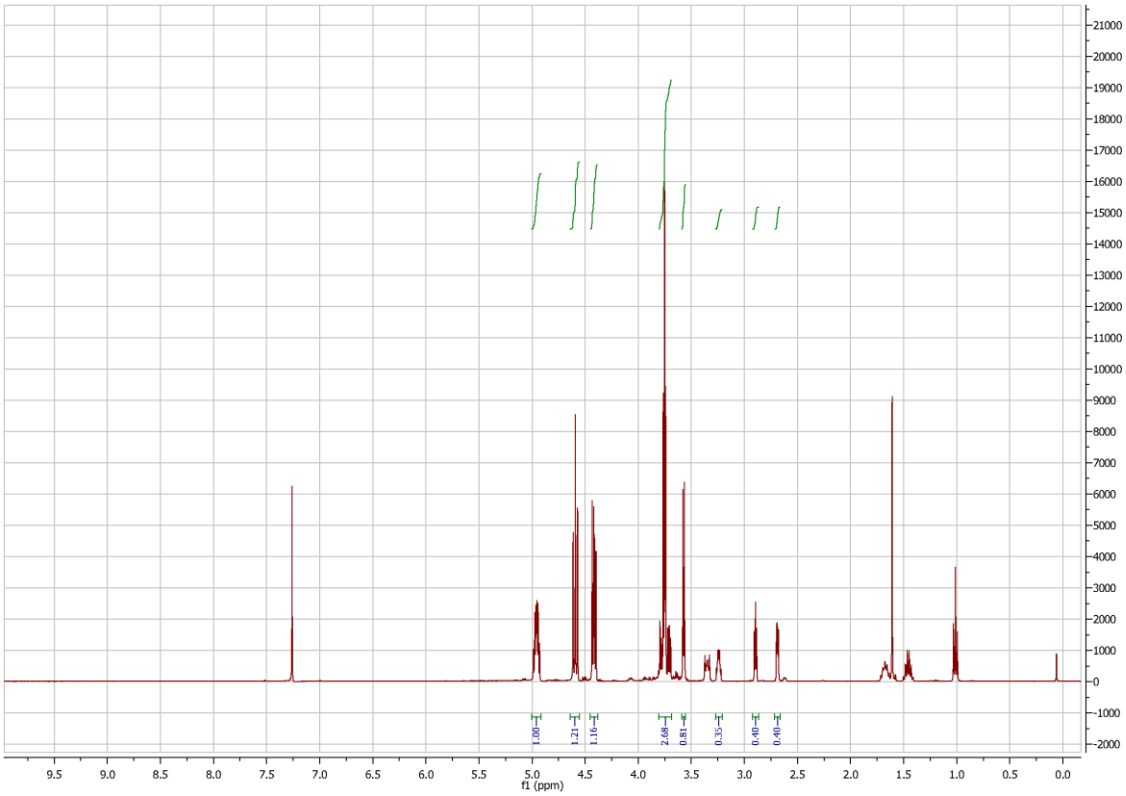

Table 2, Entry 8 epoxide **1a**, 50 % CO_2 in O_2, 24 h, Catalyst: YCl_3/TBAB (Double catalyst loading)

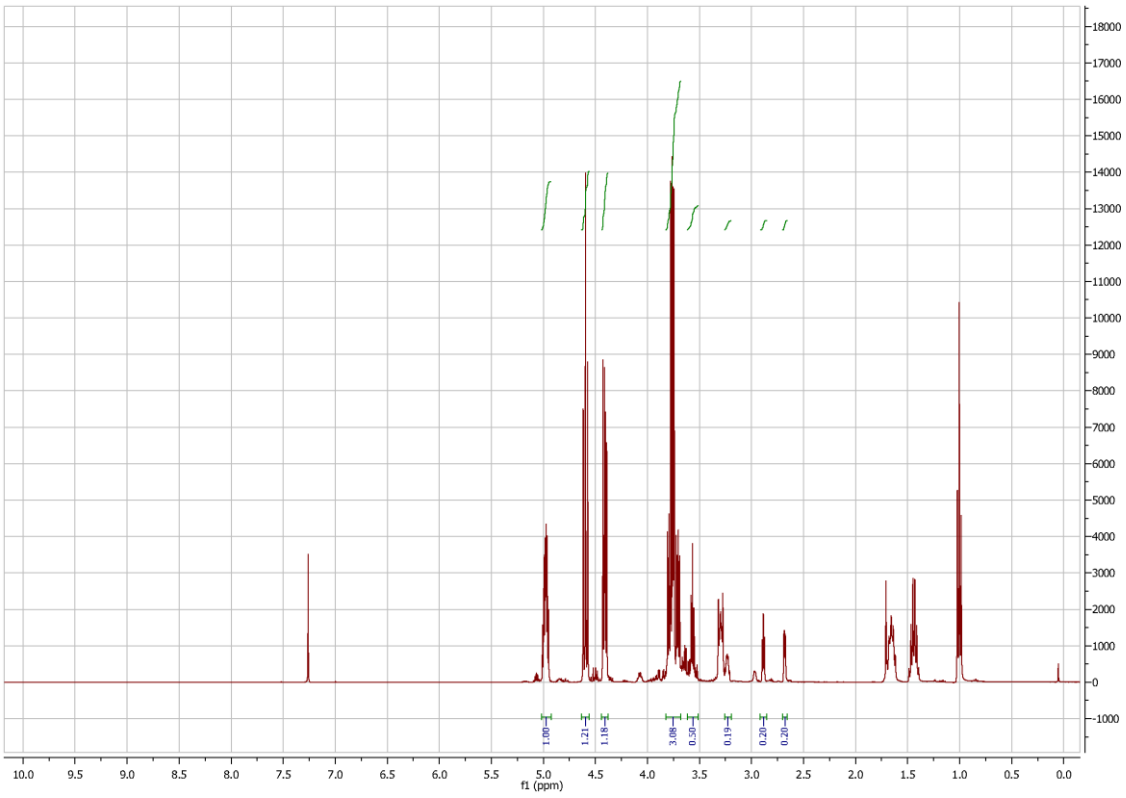

Table 2, Entry 9 epoxide **1a**, 50 % CO_2 in O_2, 5 h, Catalyst: YCl_3/TBAB (At 40 °C)

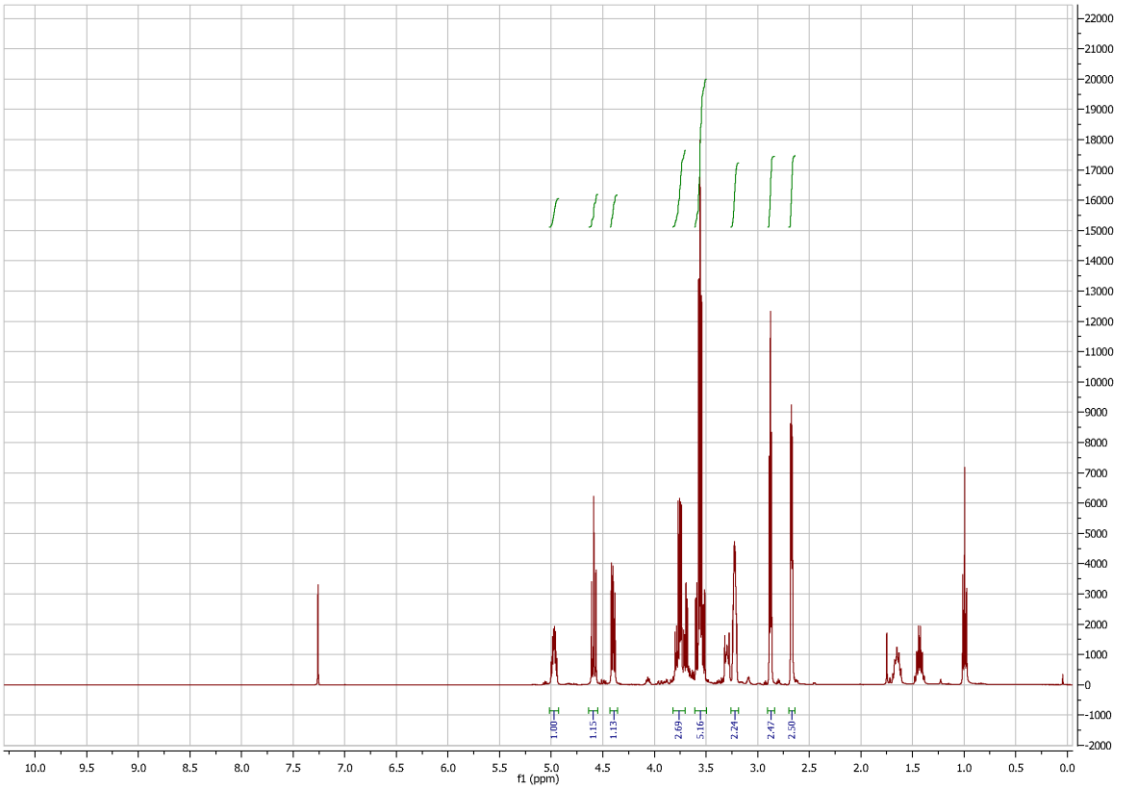

Table 2, Entry 11 epoxide **1a**, 25 % CO_2 in O_2, 5 h, Catalyst: YCl_3/TBAB

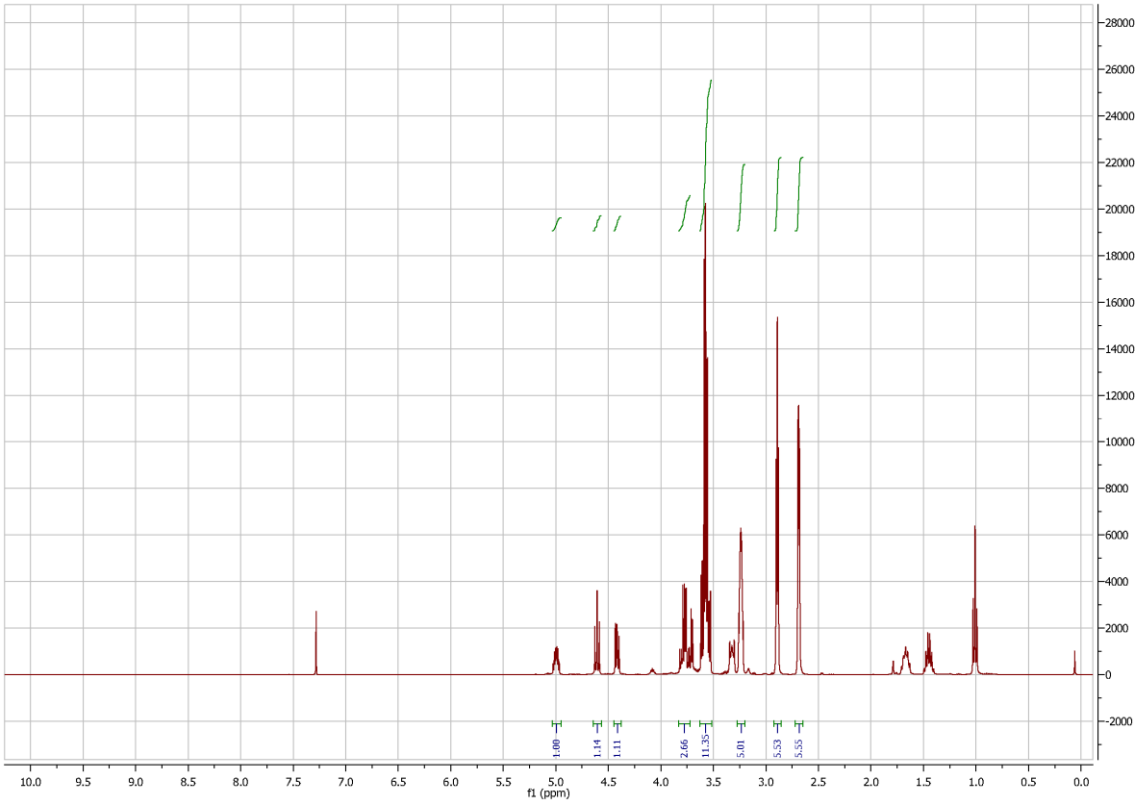

Table 2, Entry 12 epoxide **1b**, 25 % CO_2 in O_2, 5 h, Catalyst: YCl_3/TBAB

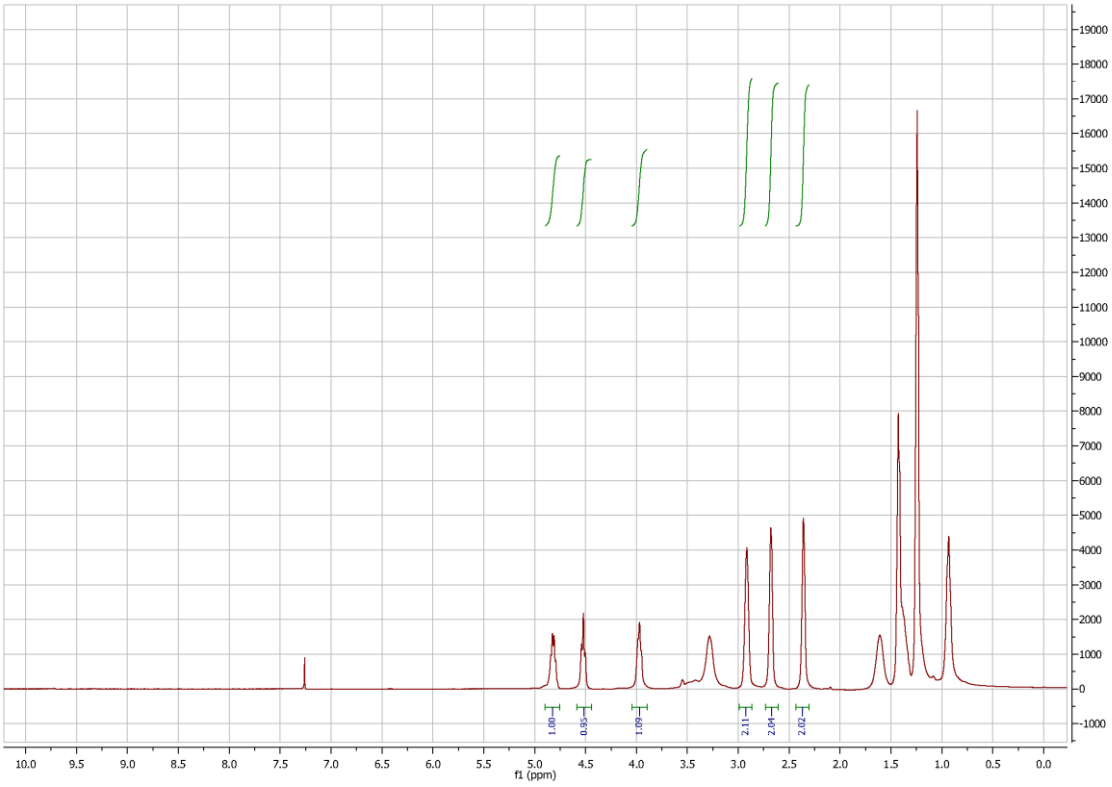

Table 2, Entry 13 epoxide **1a**, 12.5 % CO_2 in O_2, 5 h, Catalyst: YCl_3/TBAB

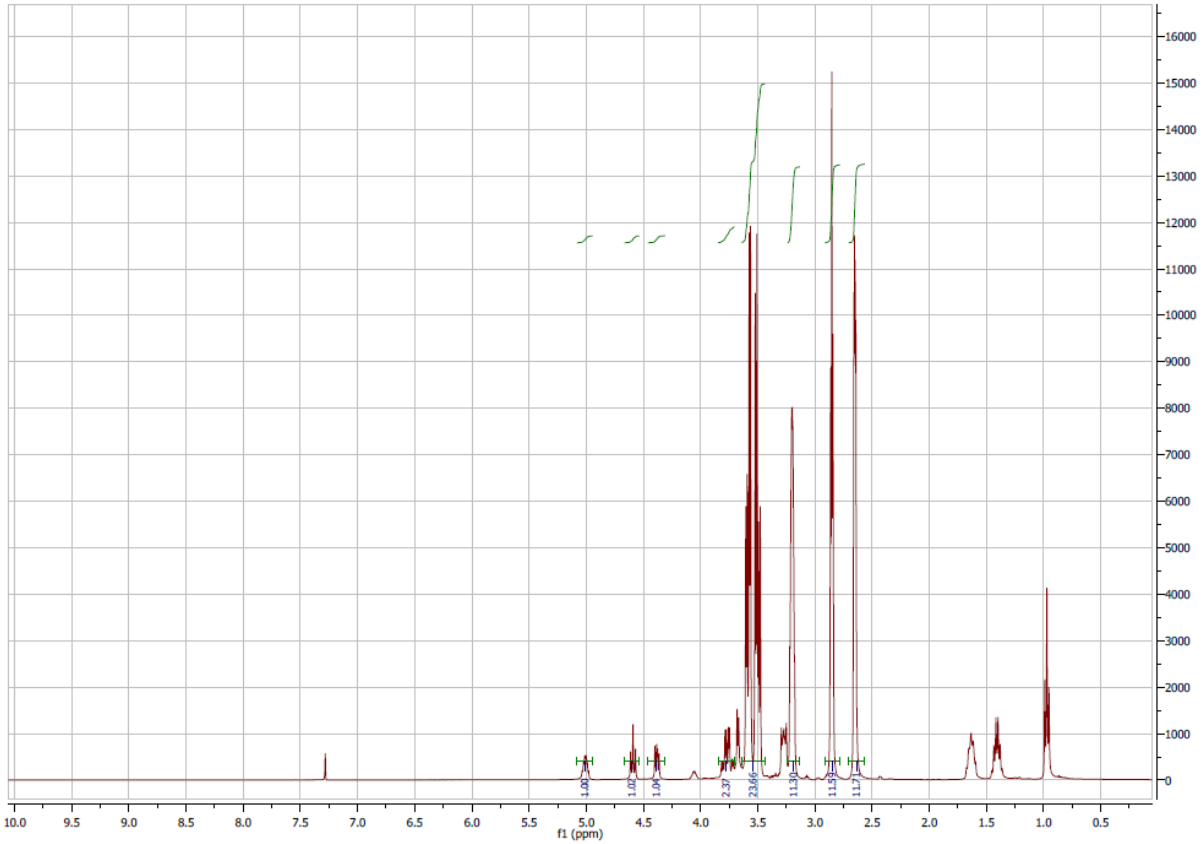

Table 2, Entry 14 epoxide **1b**, 12.5 % CO_2 in O_2, 5 h, Catalyst: YCl_3/TBAB

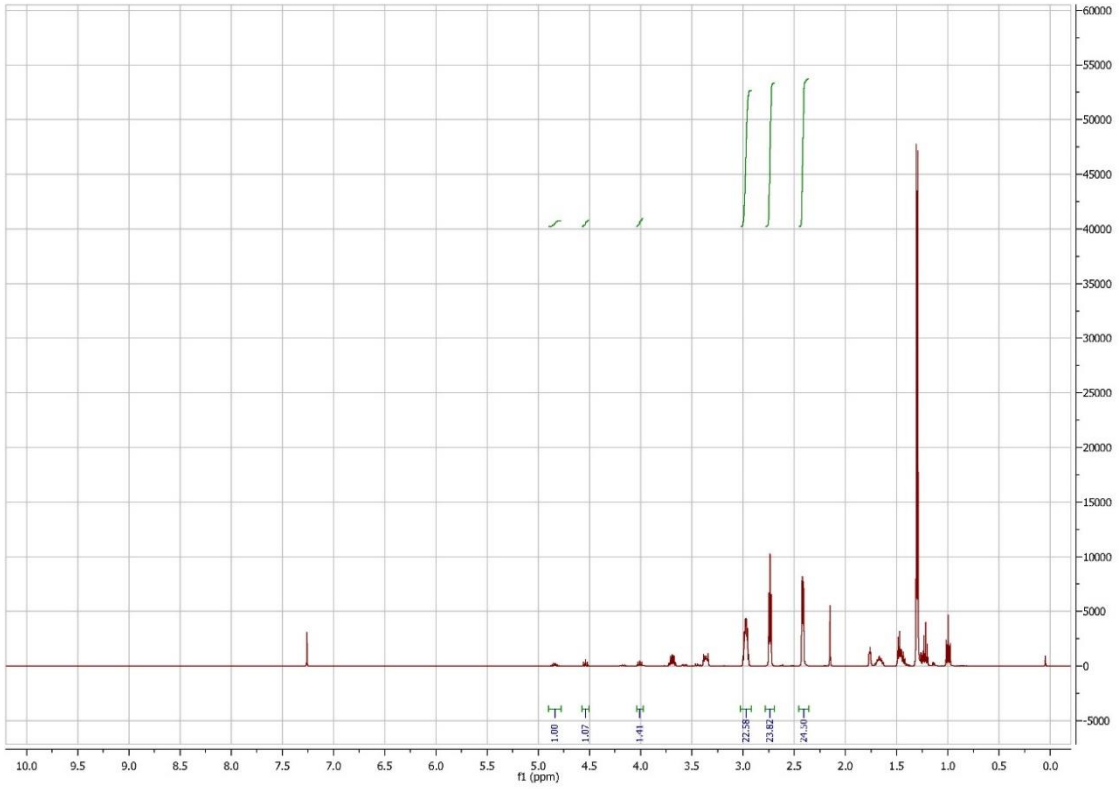

Table 2, Entry 16-f epoxide **1a**, flue gas, 5 h, Catalyst: YCl_3/TBAB

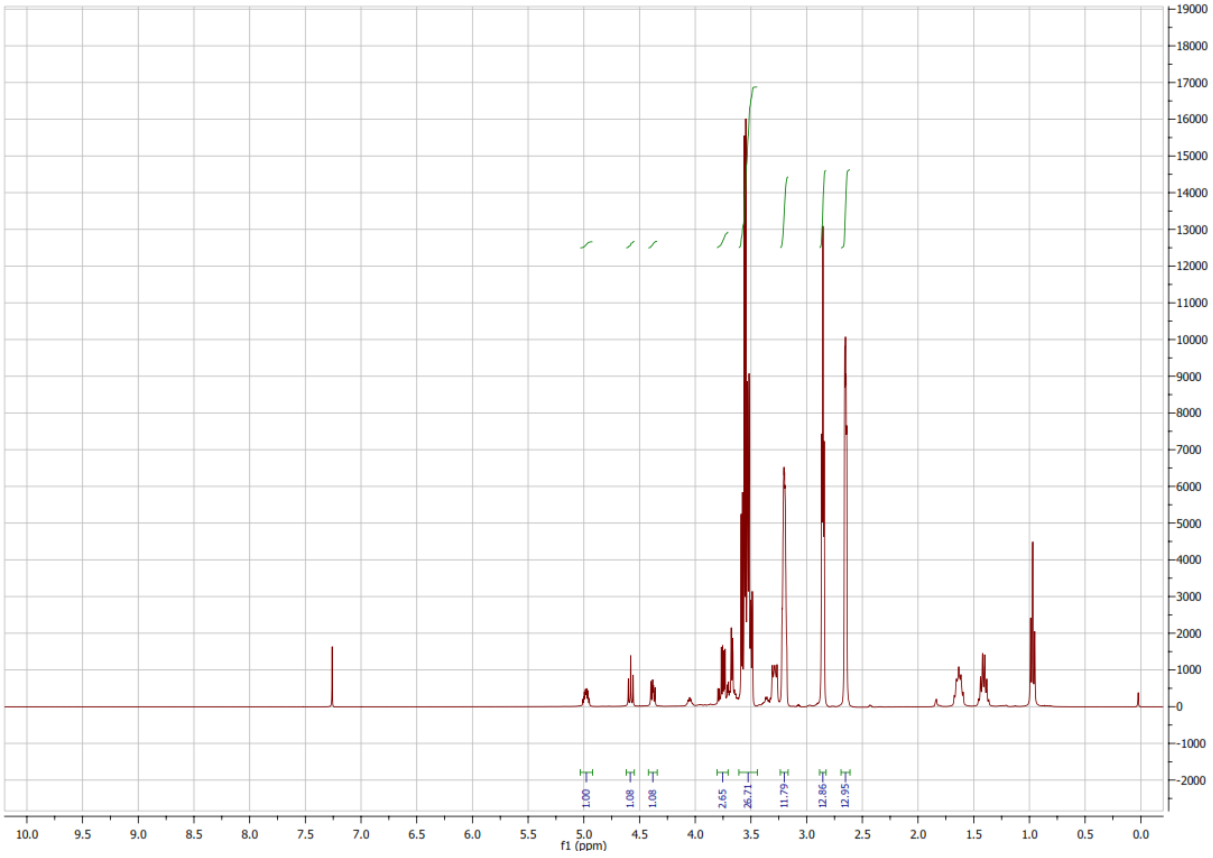

Table 2, Entry 17-f epoxide **1a**, flue gas, 5 h, Catalyst: YCl_3/TBAB

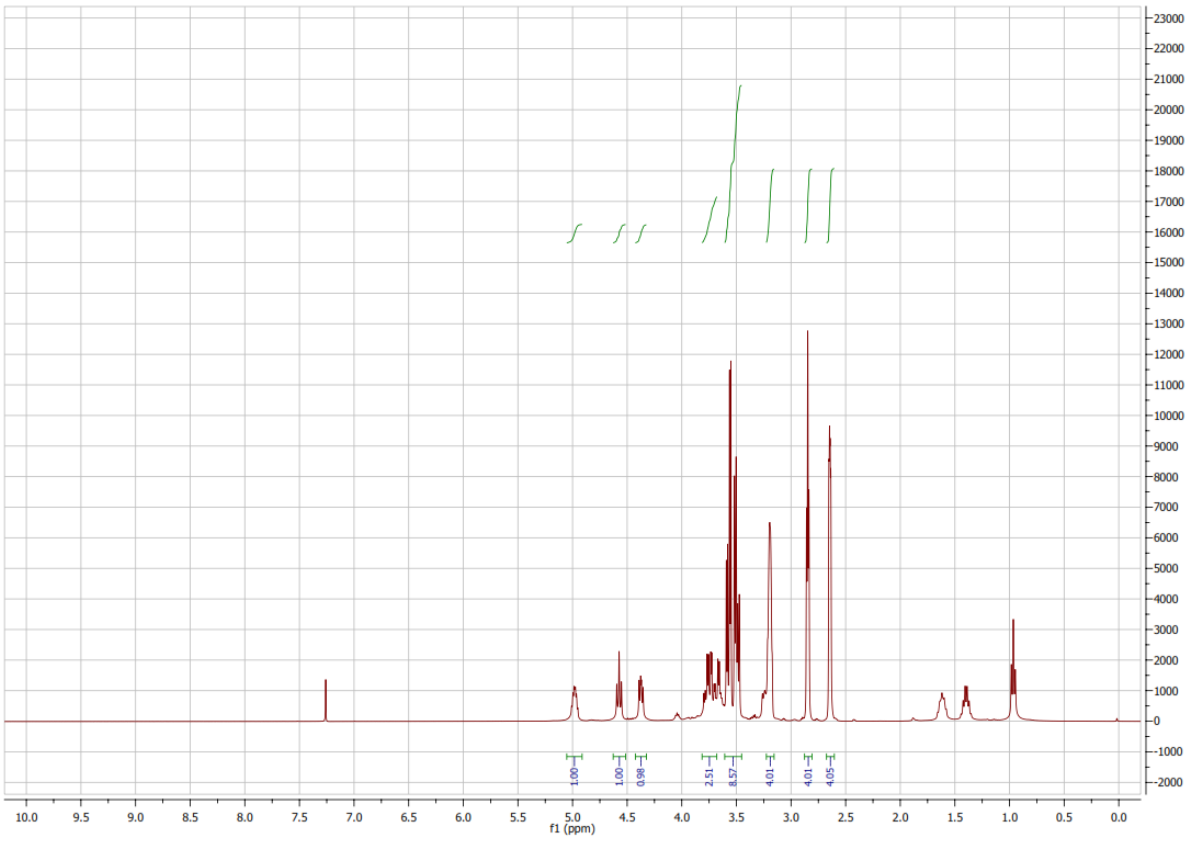

Table 2, Entry 18-f epoxide **1a**, flue gas, 5 h, Catalyst: YCl_3/TBAB (Batch reaction, 110 °C, 4 bar)

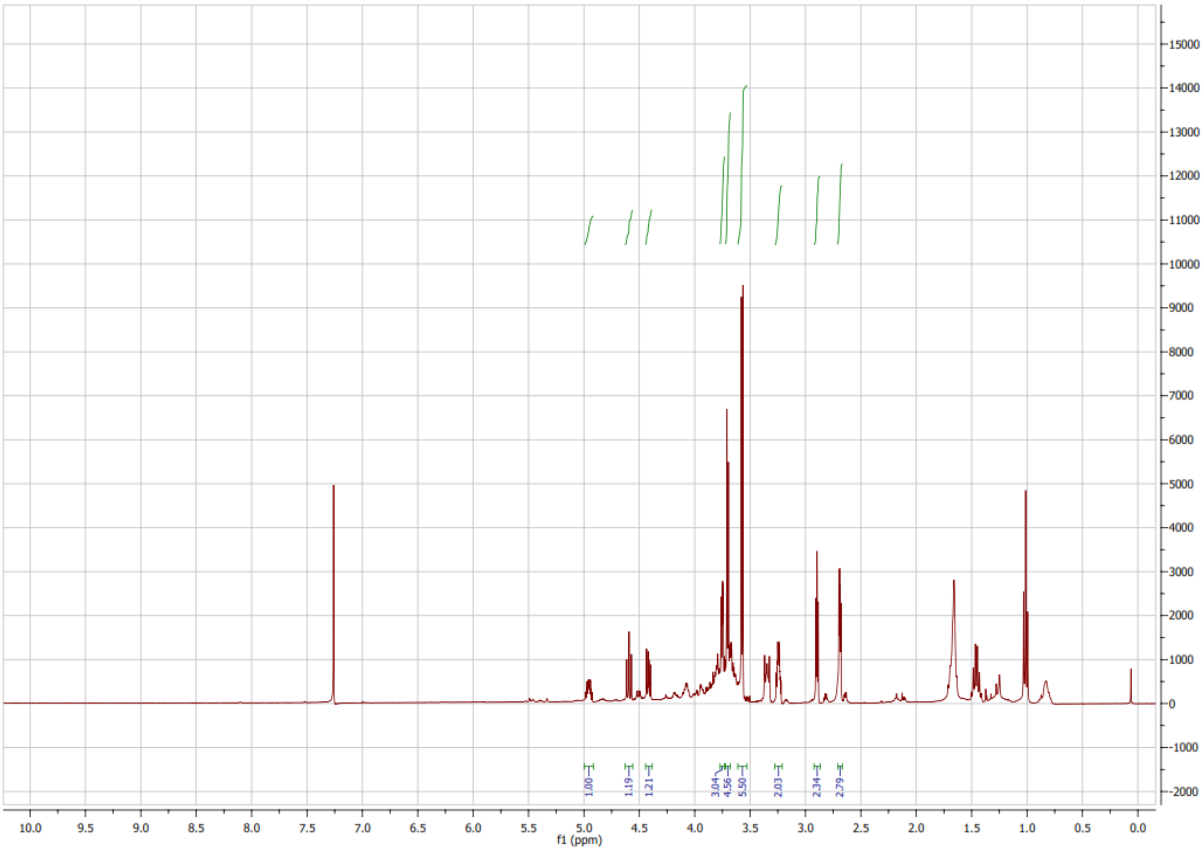

Table 2, Entry 19-f epoxide **1b**, flue gas, 5 h, Catalyst: YCl_3/TBAB (Crude spectrum)

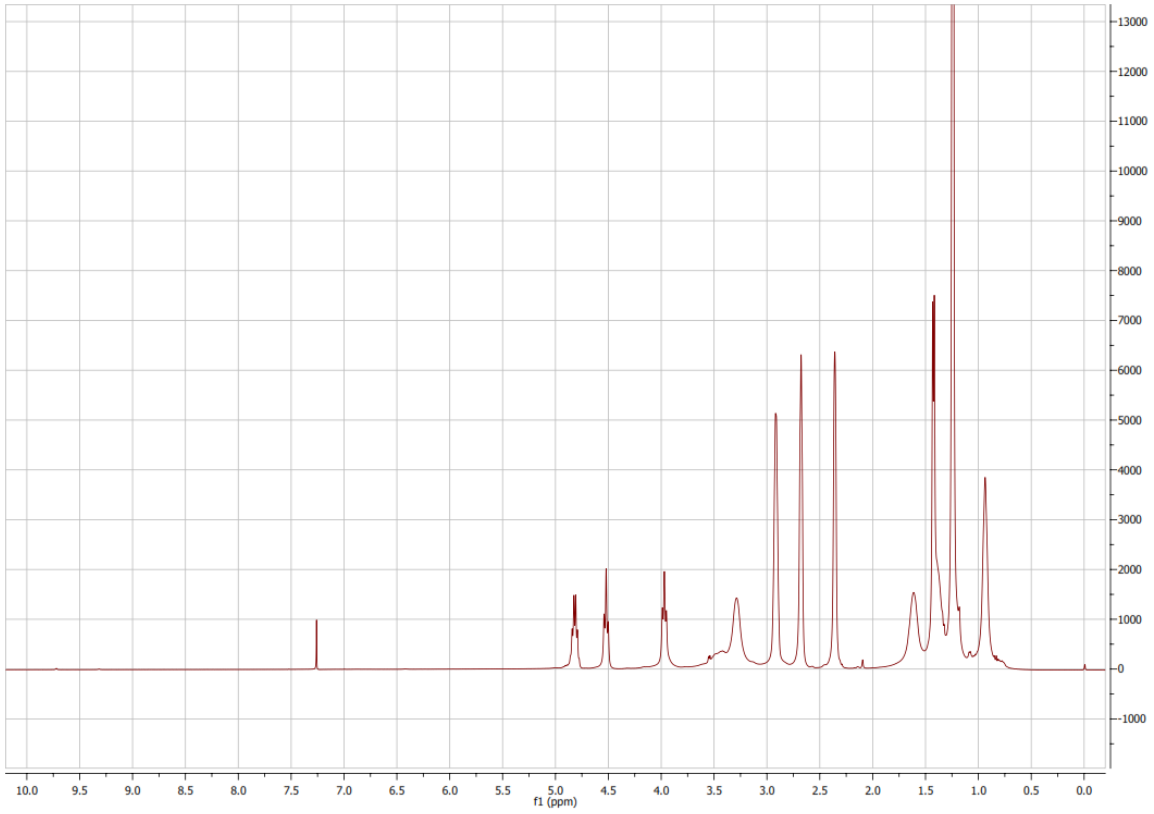

Table 2, Entry 19-f epoxide **1b**, flue gas, 5 h, Catalyst: YCl_3/TBAB (After work up: evaporation of the residual PO; addition of 3.5 mL (50 mmol) of PO as an internal NMR standard).

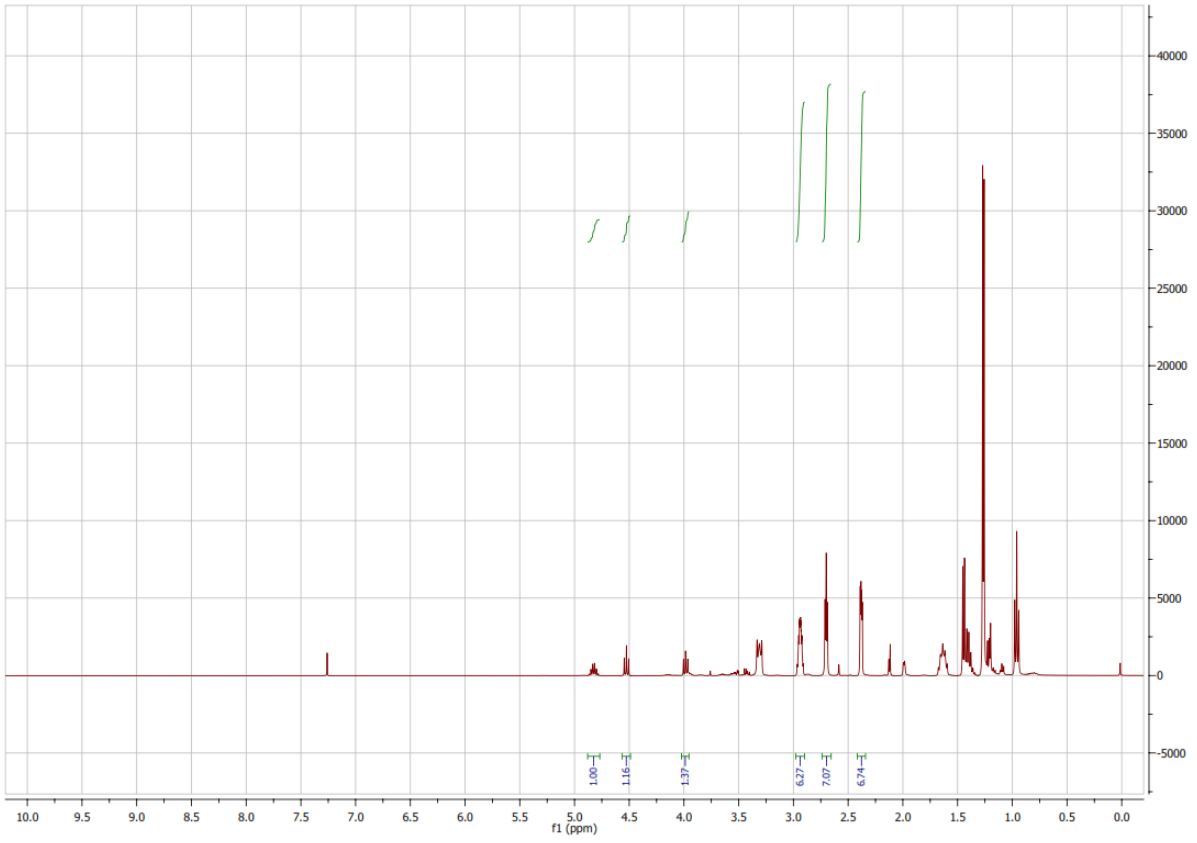

8. Supporting References

S1) See the supporting information of: A. Monassier, V. D'Elia, M. Cokoja, H. Dong, J. D. A. Pelletier, J.-M. Basset and F. E. Kühn, *ChemCatChem*, 2013, **5**, 1321-1324 (available free of charge at: http://onlinelibrary.wiley.com/store/10.1002/cctc.201200916/asset/supinfo/cctc_201200916_sm_miscellaneous_information.pdf?v=1&s=a9232f759c2db09f49ad07bff5eb347c7364f39e).

S2) See the electronic supplementary information of: B. Dutta, J. Sofack-Kreutzer, A. A. Ghani, V. D'Elia, J. D. A. Pelletier, M. Cokoja, F. E. Kühn and J. M. Basset, *Catal. Sci. Technol.*, 2014, **4**, 1534-1538 (available free of charge at: http://www.rsc.org/suppdata/cy/c4/c4cy00003j/c4cy00003j1.pdf).

S3) See the supporting information of: a) V. D´Elia, A. A. Ghani, A. Monassier, J. Sofack-Kreutzer, J. D. A. Pelletier, M. Drees, S. V. C. Vummaleti, A. Poater, L. Cavallo, M. Cokoja, J.-M. Basset and F. E. Kühn, *Chem. Eur. J.*, 2014, **20**, 11870-11882 (available free of charge at: http://onlinelibrary.wiley.com/store/10.1002/chem.201400324/asset/supinfo/chem_201400324_sm_miscellaneous_information.pdf?v=1&s=856da0b949faf2e9398269bf6c3b601f59404051).

S4) National Institute of Advanced Industrial Science and Technology (AIST): http://sdbs.db.aist.go.jp/sdbs/cgi-bin/direct_frame_top.cgi, SDBS No: 3131 (Last accessed January 2016).

S5) National Institute of Advanced Industrial Science and Technology (AIST): http://sdbs.db.aist.go.jp/sdbs/cgi-bin/direct_frame_top.cgi, SDBS No: 1949 (Last accessed January 2016).